PNAS nexus

PNAS Nexus, 2022, **1**, 1–19
https://doi.org/10.1093/pnasnexus/pgac050
Advance access publication date: 3 May 2022
Research Report

Cross-species metabolomic analysis of tau- and DDT-related toxicity

Vrinda Kalia [a], Megan M. Niedzwiecki[b], Joshua M. Bradner[a], Fion K. Lau[a], Faith L. Anderson[a], Meghan L. Bucher[a], Katherine E. Manz[c], Alexa Puri Schlotter[a], Zoe Coates Fuentes[b], Kurt D. Pennell[c], Martin Picard [d], Douglas I. Walker[b], William T. Hu[e], Dean P. Jones[f] and Gary W. Miller [a,*]

[a]Department of Environmental Health Sciences, Mailman School of Public Health, Columbia University, New York, NY, 10032 USA
[b]Department of Environmental Medicine and Public Health, Icahn School of Medicine at Mount Sinai, New York, NY, 10029 USA
[c]School of Engineering, Brown University, Providence, RI, 02912 USA
[d]Department of Neurology, Department of Psychiatry, Columbia University Irving Medical Center, New York, NY, 10032 USA
[e]Department of Neurology, Rutgers Biomedical and Health Sciences, New Brunswick, NJ, 08901 USA
[f]Division of Pulmonary, Allergy and Critical Medicine, Department of Medicine, School of Medicine, Emory University, Atlanta, GA, 30322 USA
*To whom correspondence should be addressed: Email: gm2815@columbia.edu
Edited By: Sandro Galea

Abstract

Exposure to the pesticide dichlorodiphenyltrichloroethane (DDT) has been associated with increased risk of Alzheimer's disease (AD), a disease also associated with hyperphosphorylated tau (p-tau) protein aggregation. We investigated whether exposure to DDT can exacerbate tau protein toxicity in *Caenorhabditis elegans* using a transgenic strain that expresses human tau protein prone to aggregation by measuring changes in size, swim behavior, respiration, lifespan, learning, and metabolism. In addition, we examined the association between cerebrospinal fluid (CSF) p-tau protein—as a marker of postmortem tau burden—and global metabolism in both a human population study and in *C. elegans*, using the same p-tau transgenic strain. From the human population study, plasma and CSF-derived metabolic features associated with p-tau levels were related to drug, amino acid, fatty acid, and mitochondrial metabolism pathways. A total of five metabolites overlapped between plasma and *C. elegans*, and four between CSF and *C. elegans*. DDT exacerbated the inhibitory effect of p-tau protein on growth and basal respiration. In the presence of p-tau protein, DDT induced more curling and was associated with reduced levels of amino acids but increased levels of uric acid and adenosylselenohomocysteine. Our findings in *C. elegans* indicate that DDT exposure and p-tau aggregation both inhibit mitochondrial function and DDT exposure can exacerbate the mitochondrial inhibitory effects of p-tau aggregation. Further, biological pathways associated with exposure to DDT and p-tau protein appear to be conserved between species.

Keywords: *C. elegans*, DDT, Alzheimer's disease, tau protein, metabolomics

Significance Statement:

Genome-wide association studies indicate that genetic variation is only a minor contributor to Alzheimer's disease, revealing the importance of environmental drivers of the disease. Our research indicates that the legacy pesticide dichlorodiphenyltrichloroethane (DDT) is associated with Alzheimer's disease and exposure to DDT exacerbates aggregating tau protein toxicity in the nematode model, *Caenorhabditis elegans*. Further, several metabolites and pathways associated with aggregating tau protein are conserved between humans and *C. elegans*. Our findings indicate that despite their ban, persistent chemicals in our environment can still contribute to or exacerbate pathogenesis of Alzheimer's disease and other neurodegenerative diseases.

Introduction

In 2014, 5 million people in the United States were living with Alzheimer's disease (AD). By 2060, this number is projected to grow to 13.9 million (1). Clinically, AD manifests as dementia, a progressive deterioration of memory and cognitive function (2). Pathologically, AD is characterized by severe neuronal loss, aggregation of amyloid-β (Aβ) in extracellular senile plaques, and formation of intraneuronal neurofibrillary tangles consisting of hyperphosphorylated tau (p-tau) protein whose levels can be measured in the cerebrospinal fluid (CSF). There is evidence that AD may be a metabolic neurodegenerative disease (3) as it has been associated with altered local and peripheral metabolism in several studies. Through in vitro, animal model, and epidemiological studies, investigators have found associations between tau neurofibrillary tangles and impaired glucose metabolism (4–6), altered mitochondrial trafficking, morphology and bioenergetics, and reduced ATP production (7). While aging is the strongest risk factor of AD, evidence of risk factors for dementias show that lifestyle choices and the environment may modify disease onset and alter the projected prevalence (8). Indeed, using untargeted

Competing Interest: The authors declare no competing interest.
Received: September 27, 2021. **Accepted:** April 28, 2022

high-resolution mass spectrometry based metabolomics (HRMS-metabolomics), our group has uncovered plasma derived metabolites from endogenous and exogenous sources associated with the disease (9, 10). If causally associated with the disease, these metabolites may be modified or targeted to alter disease prevalence or progression.

The role of the environment in AD pathogenesis has a controversial history (11), but recent studies provide evidence of environmental chemical exposures influencing disease risk. In a cross-sectional, case-control study, Richardson and colleagues found that cases of AD had higher levels of a metabolite of the pesticide DDT (1,1,1-tricholoro-2,2-bis(p-chloro-phenyl) ethane) in their serum (12). DDT is a highly persistent, synthetic organochlorine pesticide used for pest control in agricultural settings and to control vectors that can cause diseases like malaria and typhus. It was widely used in the United States from 1939 to 1972, until its use was banned by the US Environmental Protection Agency (EPA) (13). Despite its regulation, DDT and its metabolites remain persistent and can be detected in the blood of most of the US population (14). Additionally, DDT can be passed through breastmilk to infants, exposing generations that have been born after its ban (15). DDT is still used for vector control in some African and south Asian countries (16) and can travel long distances through evaporation, distillation, and transport via winds and ocean currents (17). Therefore, DDT poses a threat to the health of populations living in countries where it is still produced and in countries that are further away.

Caenorhabditis elegans (*C. elegans* or worms) is a nonparasitic nematode that has long been used in neuroscience and developmental research; more recently it has been gaining popularity as an in vitro model in toxicity testing. Studies in *C. elegans* show that the toxicity ranking of several toxicants, including, but not limited to, metals, organophosphate pesticides, ∼ 60% of chemicals in the EPA's ToxCast Phase I and Phase II libraries, known or suspected developmental toxicants, and metabolic toxicants, is predictive of rat LD_{50} values (18–24). The model is inexpensive and requires minimal laboratory expertise to maintain. Several fundamental aspects of biology were discovered in *C. elegans* including apoptosis, RNAi, and miRNA. Furthermore, *C. elegans* are the first complex organism to have their genome sequenced (25), allowing access to a large library of genetic mutant strains. The long history of its use in biology and the conservation of several genes and pathways between worms and humans (26) makes the nematode model valuable for biological insight (27, 28), particularly to study gene–environment interactions. In this study, we used a transgenic *C. elegans* strain that expresses human tau protein and a mutated tau protein sequence that has a propensity to form tau protein aggregates. We also used a transgenic strain to serve as control for the aggregating strain that expresses the same human tau protein but the mutated tau protein sequence is not prone to aggregation. These transgenes are expressed in all neurons of the worm driven through the *rab-3* promotor (29).

We used untargeted liquid chromatography (LC) HRMS to identify plasma and CSF metabolites associated with CSF p-tau levels of individuals from a clinical study of AD. While frontotemporal lobar degeneration with tau-immunoreactive lesions (i.e. tauopathies) also have hyperphosphorylated tau in the brain, AD has the greatest lesional burden, which correlates with CSF p-tau levels (30). We then compared metabolites associated with p-tau in the clinical study to the metabolic profile of the mutant tau transgenic strain of *C. elegans* to find metabolic features similarly affected by tau protein toxicity in humans and *C. elegans*. Finally, we tested the effect of (1) tau protein toxicity, (2) exposure to DDT, and (3) the interaction between DDT and tau protein toxicity on growth, behavior, metabolism, learning, and survival in *C. elegans*.

Materials and Methods

Chemicals

BD Bacto dehydrated agar, salts to make M9 buffer (monobasic potassium phosphate, dibasic sodium phosphate, sodium chloride, and magnesium sulfate), 1N sodium hydroxide, p, p'-DDT (> 95%), dimethyl sulfoxide (DMSO, 99.9%), acetone (99.8%, HPLC grade), n-hexane (> = 99%), dichloromethane (99.8%, HPLC grade), sodium azide (99%), and 2-butanone (≥ 99.0%) were purchased from Fisher Scientific (Waltham, MA). Carbonyl cyanide 4-(trifluoromethoxy) phenylhydrazone (FCCP, > 98%) was purchased from Sigma-Aldrich (St. Louis, MO). Certified reference standards for gas chromatography (GC)-HRMS quantification were purchased from Accustandard (New Haven, CT), including o, p'-DDT, p, p'-DDT, o, p'-DDE, p, p'-DDE, $^{13}C_{12}$ labeled p, p'-DDE, D_8 labeled p, p'-DDT, phenanthrene D-10, and chrysene D-12. The hypochlorite solution used for synchronization was prepared using household bleach (Clorox, 8% sodium hypochlorite), water, and 1N sodium hydroxide.

Human: participants and sample collection

This study was approved by the Emory University Institutional Review Board and the methods have been previously described (9). Briefly, subjects were recruited from the Emory Cognitive Neurology Clinic and the Emory Alzheimer's Disease Research Center. Each subject underwent a detailed neurological and neuropsychological evaluation. Subjects were classified as having normal cognition (NC) if there was no subjective cognitive complaint and neuropsychological analysis showed normal cognitive functioning for their age, gender, education, and race; mild cognitive impairment (MCI) (31), or AD dementia (32) according to NIA-AA criteria (9). Plasma and CSF samples were collected and processed as described previously (9, 33). CSF AD biomarker analysis was performed as previously described using a Luminex 200 platform to determine levels of total tau (t-Tau), and tau phosphorylated at threonine 181 (p-Tau_{181}) (34).

Caenorhabditis elegans methods

Caenorhabditis elegans: growth and maintenance

Standard methods of culture, including the use of normal or high growth media (NGM/HGM) plates, culture temperature of 20°C, and the OP50 *Escherichia coli* strain as a food source, were followed as described (27) unless noted otherwise. *Caenorhabditis elegans* strains used included the wild type N2 Bristol strain, BR5271 (*byIs162* [$P_{rab\text{-}3}$::F3(delta)K280 I277P I380P + $P_{myo\text{-}2}$::mCherry]; referred to as the "non-aggregating/non-agg" strain), and BR5270 (*byIs161* [$P_{rab\text{-}3}$::F3(delta)K280 + $P_{myo\text{-}2}$::mCherry]; referred to as the "aggregating/agg" strain). All strains were provided by the Caenorhabditis Genetics Center, which is funded by NIH Office of Research Infrastructure Programs (P40 OD010440).

Caenorhabditis elegans: exposure to DDT

Worms were exposed to the pesticide p, p'-DDT or the solvent control, DMSO, on NGM plates. DDT exposure plates were created using methods previously described (35). Briefly, a 20 mM stock of DDT, made by dissolving in 100% DMSO, was diluted to 150 μM with sterile water and then applied on the surface of NGM plates

spotted with OP50 *E. coli* to obtain the appropriate final concentration of DDT on the plate. The solvent control plates were created following the same dilution but without DDT to achieve a final concentration of 0.015% DMSO. DDT was allowed to diffuse and the plates were allowed to equilibrate for 2 hours before worms were introduced. All worms were exposed to a final concentration of 3 μM DDT unless otherwise stated.

Caenorhabditis elegans: DDT uptake experiments

A synchronized population of wildtype worms, created using hypochlorite treatment, were grown on 10 cm NGM plates with 0.3, 3, or 30 μM DDT, and the DMSO control. The nonaggregating and aggregating worms were similarly synchronized and exposed to 3 μM DDT or DMSO. All strains were collected after 72 hours of exposure, at the young adult stage. They were washed in M9 buffer 4x and sorted into aliquots of 1,000 to 1,200 worms using the COPAS FP-250. The volume of M9 buffer in each sample was reduced to 100 μL and each sample was snap frozen in liquid nitrogen. To extract DDT and its metabolites, the worm cuticle was disrupted by bead beating (6.5 m/s for 1 min) and the samples were analyzed for levels of DDT using GC-HRMS.

Caenorhabditis elegans: growth determined through size measured on COPAS Biosorter

The COPAS Flow Pilot (FP) 250 is an instrument used for high-throughput manipulation of *C. elegans*. For each worm that passes through the flow cell, the COPAS FP-250 determines its time-of-flight (TOF), which represents the length of the worm passing through the flow cell, and the extinction, which represents the optical density or thickness of the worm passing through the flow cell. After hypochlorite synchronization, eggs from all three strains were allowed to hatch and develop on 10 cm NGM plates with 3 μM DDT or DMSO. Worms were sorted through the COPAS FP 250 to measure TOF and extinction 46 to 50 hours after synchronization (around the L4 stage, $n = 1{,}000$ to 4,000 per group, object inclusion criteria: Log(TOF) > 6 and Log(extinction) > 5) and at 70 to 72 hours post synchronization (young adults, $n = 1{,}000$ to 4,000 per group, object inclusion criteria: Log(extinction) between 5.5 and 9). We used inclusion criteria that have been previously estimated for the L4 larval and adult stage on the COPAS FP-250 (18). Measures of TOF and extinction were compared across the strains and treatment groups using a two-way analysis of variance with an interaction term at each time point.

Egg-laying behavior

Following the 72-hour DDT exposure period, day 1 adult worms, 1 per well, were transferred to 96-well plates containing 20% hypochlorite solution. Dissolution of the worm body and release of eggs was monitored and eggs were counted manually. Data were collected from four trials with 15 worms assessed from each group per trial and analyzed using a Poisson regression model with an interaction term.

Caenorhabditis elegans: swim behavior

The celeST software package was used to determine aspects of swim behavior for the different strains exposed to DDT or the solvent control (36). Briefly, three-to-four worms at the young adult stage were placed in 60 μL of M9 buffer in a 15-mm ring preprinted on a microscope slide (Fisherbrand microscope slides with two 15-mm diameter circles, catalog #22–339–408). Recordings of swim behavior were made as a series of jpeg images using a chameleon 3 camera (FLIR, Wilsonville, OR) for 30 s at a frame rate of 18 f/s. Data were collected from four-to-five trials with a total of 50 to 100 worms recorded per group.

Caenorhabditis elegans: seahorse XFe96 extracellular flux analysis

The three strains exposed to DDT or solvent control were collected at the young adult stage and washed in M9 buffer 4x for analysis using the Seahorse XFe96 extracellular flux analyzer (37). Briefly, 3 to 30 worms in M9 buffer were plated into the wells of a Seahorse utility plate and the volume of M9 buffer in each well was made up to 200 μL. M9 buffer without any worms was used as the blank for background correction. Baseline respiration was measured (measurement numbers 1 to 5), followed by injection of FCCP (10 μM, final concentration) to elicit maximal respiration (measurement numbers 6 to 14), followed by sodium azide (40 mM, final concentration) to measure nonmitochondrial respiration (measurement numbers 15 to 18). Data were normalized to the number of worms in each well to determine the rate of oxygen consumption (pmol O_2/min) per worm. Basal respiration was determined as the difference between nonmitochondrial respiration and the average OCR at measurements 2 through 5; maximal respiration was determined as the difference between nonmitochondrial respiration and the average OCR measured after the FCCP injection; and spare respiratory capacity was measured as the difference between basal and maximal respiration.

Caenorhabditis elegans: associative learning assay

The associative learning assay was carried out as previously described (38) with some modifications. The assay relies on an associative memory paradigm where worms are trained by pairing the presence of food with the odor of 10% butanone. Briefly, worms were hypochlorite synced and allowed to grow on DDT or solvent control plates for about 72 hours, until they reached the young adult stage. Worms were collected off plates and washed 3x in M9 buffer. After the last wash, the naïve attraction toward butanone was assessed. Worms were then starved for an hour, after which the conditioned training was performed to pair the odor with the presence of food. The attraction toward butanone was determined just after conditioning, representing their ability to learn and form an associative memory. To count the number of worms attracted to the butanone spot or the control (95% ethanol) spot, images of the entire assay plates were taken on a Basler GigE camera, and the images were analyzed using a MATLAB algorithm created by the Murphy lab (38).

Caenorhabditis elegans: survival analysis

Wildtype worms and the transgenic strains were exposed to DDT or DMSO until the young adult stage, around 72 hours. After exposure, worms were collected off plates and washed in M9 buffer four times. We created four replicates per treatment group per strain with 25 to 35 worms each. Adult worms were counted and transferred everyday onto new 6 cm NGM plates until they stopped producing progeny (~ adult day 6). At this point, worms were transferred onto 6-cm NGM plates with nystatin and ampicillin. Worms were then counted every other day and scored as dead if they did not respond to the gentle touch of a platinum wire. A worm was censored from the plate if it was missing, showed internal hatching, or was damaged during transfer. Data was analyzed using Kaplan–Meier survival calculations and a cox proportional hazards model to test for interaction between strain and DDT exposure using the R package survival.

HRMS methods

GC-HRMS for C. elegans DDT uptake

Worm tissue concentrations of p, p'-DDT, p, p'-DDE, p, p'-DDD, o, p'-DDT, o, p'-DDE, and o, p'-DDD were measured using methods previously described (39). Prior to extraction, each sample was spiked with labeled isotope internal standards to assess analyte recovery. Each sample was extracted using QuEChERS (Quick, Easy, Cheap, Effective, Rugged, Safe) (40). The samples were first vortex mixed in centrifuge tubes with 1 mL 1:1:1 hexane:acetone:dichloromethane and sonicated for 30 min. The entire sample and the supernatant were transferred to a centrifuge tube containing 150 g MgSO4 and 50 mg C18 (United Chemical Technologies, Bristol, PA), vortexed for 30 s, and centrifuged for 5 min at 1,105 × *g*. This extraction was repeated 2 more times and the final 3 mL extract was evaporated to 150 μL under nitrogen (Organomation 30 position Multivap Nitrogen Evaporator), transferred to a low-volume (300 μL) GC vial, and spiked with phenanthrene-D10 and chrysene-D12 as volumetric internal standards to ensure injection consistency during GC-HRMS analysis. Extracts were analyzed on a GC Q-Exactive Orbitrap MS (Thermo Scientific) equipped with a Thermo Trace 1300 gas chromatograph and TriPlus RSH Autosampler using chromatographic methods described previously (Elmore et al. 2020). The MS was operated in full scan mode, with a scan range of 50 to 750 m/z. Analytes were quantified using the most abundant fragment and identity was confirmed using the ratio of two confirming ions and retention times (Table S1, Supplementary Material).

Sample preparation for LC high resolution mass spectrometry (LC-HRMS)

Human sample preparation: samples were prepared for HRMS-metabolomics using methods detailed elsewhere (9, 41–43). Briefly, aliquots of plasma or CSF were removed from −80°C storage and thawed on ice. A volume of 65 μL of each biofluid was added to 130 μL of acetonitrile containing a mixture of stable isotopic standards, vortexed, and allowed to equilibrate for 30 min. Proteins were precipitated by centrifuge (16,100 × *g* at 4°C for 10 min) and the supernatant was transferred to a low-volume vial for analysis.

Caenorhabditis elegans sample preparation: two different experiments were conducted and prepared: (1) to determine the metabolic effects of aggregating tau protein, a synchronized population of worm eggs of the nonaggregating and aggregating strain were allowed to hatch and grow on NGM plates. (2) To determine the effect of DDT on metabolism in all strains, a synchronized population of all strains, wildtype, nonaggregating, and aggregating worms, were placed on NGM plates coated with DDT or DMSO. In both experiments, worms were allowed to grow until larval stage 4. For collection, worms were washed 4x in M9 buffer and sorted into four-to-six replicates containing 500 worms using a COPAS FP-250. The final volume was reduced to 100 μL by centrifuge and each sample was snap frozen in liquid nitrogen and stored at −80°C until needed for processing. Metabolites were extracted using methods described previously (44, 45). Briefly, two volumes of acetonitrile (200 μL) containing a mixture of internal standards was added to the 100μL worm suspension, and samples were homogenized by bead-beating. A spatula-full of zirconium oxide beads (~10 beads, 0.5 mm diameter, Yttria stabilized) from Next Advance (Troy, NY) was added to each worm sample, and placed in a bead beater (Next Advance Bullet Blender Storm, Troy, NY) set at 6.5 m/s for 30 s. Extracts were then allowed to equilibrate on ice for 1 min, and placed in the beater for another 30 s at the same speed. After equilibration on ice for 30 min, proteins were removed by centrifuge (15,000 × *g* at 4°C for 10 min). All sample processing was performed on ice or in a cold room when necessary.

High-resolution metabolomic analyses

Human sample extracts were analyzed by reverse-phase C18 LC (Dionex Ultimate 3000) and Fourier transform mass spectrometry in positive electrospray ionization (ESI) mode, resolution (FWHM) of 70,000 (9). Sample extracts from *C. elegans* were analyzed on an LC-HRMS platform in two ways: (1) for determination of the effect of aggregating tau protein on metabolism, sample extracts were analyzed using untargeted LC-HRMS using methods described previously (46). Mass spectral data were generated under positive electron spray ionization in full scan mode. (2) Due to changes in LC-HRMS technologies, analysis of DDT exposure studies used slightly different analytical conditions; however, detection of endogenous metabolites across the two platforms is consistent. For determination of the effect of DDT on metabolism in all strains, after processing, the supernatant was diluted 1:1 in HPLC-grade water and analyzed using a HILIC column (positive and negative ESI mode) and C18 column (positive and negative ESI mode). Separation was similar to conditions described above, except an acetonitrile gradient with 10 mM ammonium acetate was used for HILIC, and acetonitrile gradient with 0.5% acetic acid for C_{18}. For both methods, 10 μL of the sample extract was injected in triplicate. All mass spectral data were generated on an Orbitrap mass spectrometer in full scan mode (1: Thermo Scientific Q-Exactive HF and 2: Thermo Scientific HFX), scanning for mass range 85 to 1,250 m/z. All raw mass spectral data were extracted using the R packages apLCMS (47) and xMSanalyzer (48). Due to the need for multiple batches in the human study, batch correction was performed using ComBat (49). No batch effects were observed for *C. elegans* studies and detected intensities were used as is for statistical analyses. Intensities were generalized log transformed prior to analysis.

High-resolution metabolomic data analyses

Human: analysis of LC-HRMS data

Association of metabolite peaks with p-tau levels were assessed using linear regression for metabolites detected in > 80% of study samples while controlling for sex, age, and analysis batch. Features associated with p-tau levels ($P < 0.05$) were analyzed for metabolic pathway enrichment using mummichog (version 2.0.6) in Python (version 2.7) (50).

In a sensitivity analysis, features associated with AD dementia vs. NC were examined using the subset of features present in > 20% of samples, reflecting a markedly lower threshold for feature filtering compared to our previous analysis of AD (9). Statistical analyses to determine plasma metabolomic features associated with AD were conducted as previously described (9). The relationship between the metabolite putatively identified as a DDT metabolite and plasma and CSF metabolomics was assessed using linear regression while controlling for the effect of sex, age, and batch of analysis. Features associated with the DDT metabolite ($P < 0.05$) were also analyzed for metabolic pathway enrichment.

Caenorhabditis elegans: analysis of LC-HRMS data and overlap

All feature tables were processed as follows: first, the intensity of a metabolite peak in the samples was compared to

Table 1. Demographic data of patients. Patients with a diagnosis of AD or MCI were included in the analysis. Of these patients, 142 plasma and 78 CSF samples were analyzed using the LC-HRMS method. t-Tau: total tau protein; p-Tau181: tau phosphorylated at threonine 181.

	Control	AD	MCI
PLASMA (N)	46	51	45
% Male	30	35	48
Age (y, mean ± SD)	66.5 ± 8.7	65.9 ± 8.9	69.4 ± 6.6
CSF t-Tau (pg/mL, mean ± SD)	44 ± 23	120 ± 66	76 ± 70
CSF p-Tau181 (pg/mL, mean ± SD)	32 ± 14	74 ± 30	51 ± 25
CSF (N)	25	26	27
% Male	28	38	55
Age (y, mean ± SD)	66.2 ± 8.2	64.8 ± 8.2	70.2 ± 6.2
CSF t-Tau (pg/mL, mean ± SD)	44 ± 24	113 ± 64	69 ± 44
CSF p-Tau181 (pg/mL, mean ± SD)	32 ± 13	79 ± 32	53 ± 20

its intensity in the medium blank (M9 buffer). If the intensity was ≥ 1.5 times the intensity in the blank in all samples, it was retained for subsequent analysis. Second, if a metabolite peak was missing from fewer than 50% of the samples, it was replaced with half the value of the minimum intensity measured in the samples. Features missing from more than 50% of the samples were removed from downstream analysis. Third, the filtered and imputed feature table was imported into MetaboAnalyst (51) and normalized by generalized log transformation. Three different analyses were conducted using the processed *C. elegans* data:

1. Metabolic effects of aggregating tau protein. The filtered feature table was used to determine the metabolites associated with the aggregating worms by comparing aggregating to nonaggregating worms using multiple t tests. Metabolites with $P < 0.05$ were analyzed for pathway analysis using mummichog hosted on MetaboAnalyst (52) using the *C. elegans* KEGG reference map.
2. Analysis of metabolites common to humans and *C. elegans* that are associated with tau protein. Plasma and CSF derived metabolites that were associated with CSF p-tau ($P < 0.05$) or neuronal expression in *C. elegans* ($P < 0.05$) were compared using KEGG ID annotations from pathway analysis. A metabolite was considered overlapping if it was significantly associated with tau protein in both species, was annotated with a KEGG ID, and the direction of association was concordant between worms and humans.
3. The metabolic effect of DDT in all three strains. The filtered feature table was used to determine: the metabolomic profile of DDT exposure and presence of interaction between strain and DDT exposure. For all analyses, we used multiple two-way ANOVAs with interaction to compare differences in levels of each feature across the groups. Significant metabolite peaks were tested for pathway enrichment using mummichog on MetaboAnalyst and the *C. elegans* KEGG reference map.
4. Analysis of metabolites common to humans and *C. elegans* that are associated with DDT or its metabolite. Plasma and CSF metabolites that were associated with the DDT metabolite ($P < 0.05$) were compared to worm metabolites associated with DDT exposure using KEGG ID annotations from pathway analysis. A metabolite was considered overlapping if it was significantly associated with DDT in both species, was annotated with a KEGG ID, and the direction of association was concordant between worms and plasma, and between worms and CSF.

Statistical analyses

Tests for significance were determined through two-way ANOVA to test for interaction between strain and treatment, and posthoc Tukey's HSD test, unless stated otherwise. All data were analyzed in R (version 4.0.2) using RStudio (v1.1.456) unless otherwise stated.

Results

CSF and plasma metabolism associated with CSF p-tau levels

There were no significant differences in the distribution of age or gender between the three different diagnoses. Patients with AD and MCI had higher levels of p-tau measured in their CSF compared to controls (Table 1). Following data extraction and filtering, 6,028 metabolite peaks were detected and measured in the CSF of patients and 7,249 m/z features in plasma. After controlling for the age, sex, and batch of analysis, we found 225 metabolites in CSF (Fig. 1A) and 391 in plasma (Fig. 1C) that were associated with CSF levels of p-tau at $P < 0.05$. Pathway analysis of the CSF metabolites found pathways associated with glutamate metabolism, carnitine metabolism, lysine metabolism, saturated fatty acid metabolism, as well as metabolism of several amino acids (Fig. 1B), while pathways enriched by plasma-derived metabolites were consistent with drug metabolism, carnitine metabolism, lysine metabolism, and pathways associated with energy production (Fig. 1D).

Changes in global metabolism associated with aggregating tau protein expression in *C. elegans*

HRMS-metabolomics detected 19,380 metabolite peaks in *C. elegans* using the HILIC column with positive ionization mode. After blank filtration and imputation, 8,860 were retained for further analysis. Metabolome wide association analysis found more than 900 m/z features that were significantly different ($P < 0.05$) between the aggregating and nonaggregating strain (Fig. 1E). Metabolites were tested for pathway enrichment using the KEGG *C. elegans* reference map, which identified changes in the tryptophan and arginine pathway, glycerophospholipid metabolism, lysine degradation, glutathione metabolism, as well as glutamate and glutamine metabolism implicating altered amino acid metabolism (Fig. 1F).

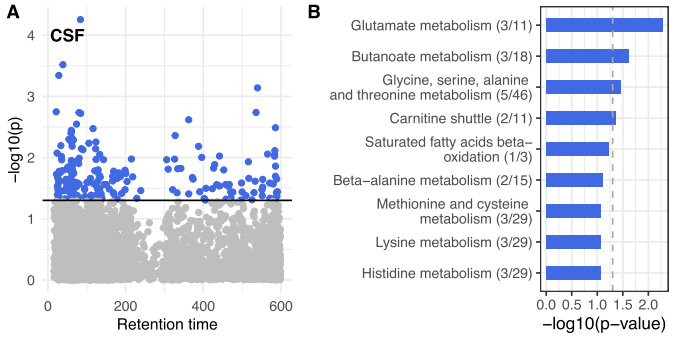

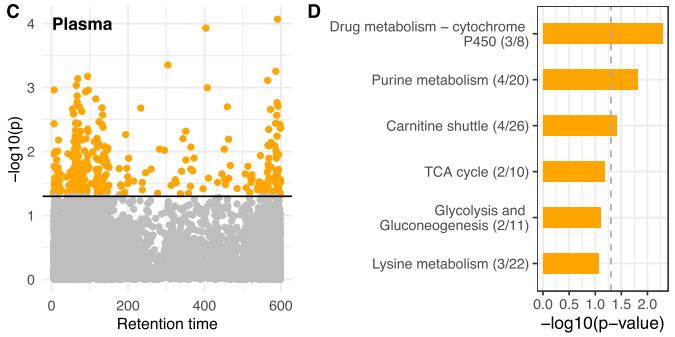

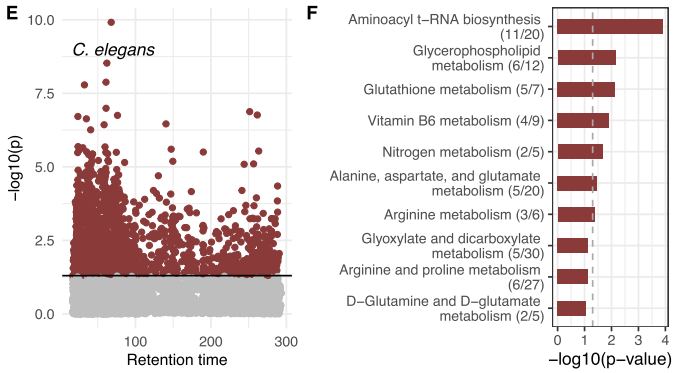

G

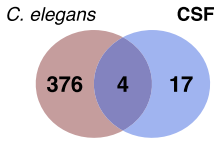

H

Annotation	Direction	KEGG ID
Tyrosine	↓	C00082
Carnitine	↓	C00487
Cystine	↓	C00491
N,N-dimethylaniline-N-oxide	↓	C01183

I

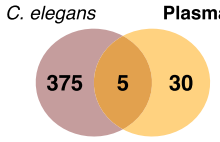

J

Annotation	Direction	KEGG ID
Lipoamide	↓	C00248
Diethylthiophosphoric acid	↓	C06607
11, 12-dihydroxy eicosatrienoic acid	↑	C14775
N-acetyl-lysine	↓	C12989
Cystine	↓	C00491

Fig. 1. Global metabolomic features associated with p-tau in humans and *C. elegans*. In (A), a metabolome-wide association study found 225 CSF metabolites associated with CSF p-tau levels with $P < 0.05$. Enriched pathways corresponding to CSF p-tau associated metabolites are shown in (B). In (C), 391 plasma metabolites were found to be associated with CSF p-tau levels, with $P < 0.05$; enriched pathways are listed in (D). The aggregating strain shows the greatest influence on the metabolome. In (E), a metabolome-wide association study found 900 metabolites significantly different between the aggregating and nonaggregating worms. These metabolites resulted in the enriched pathways shown in (F). In (G) and (I), Venn diagrams shows the overlap between annotated metabolites associated with p-tau in worms and the human matrices; (H) and (J) include the name and KEGG ID for the overlapping metabolites. The nature of the relationship between the metabolite and p-tau, whether positively associated (upward arrow) or negatively associated (downward arrow), is shown under the direction column in (H) and (J).

Table 2. Putatively identified DDT metabolite higher in people with AD. Lowering the filtering threshold revealed a positive association between a putative DDT metabolite and risk of AD. [a]ID level indicates annotation confidence: (1) m/z and retention time confirmed with MS2, (2) multiple/isotopes present; (3) m/z matched single adduct mass within 10 ppm mass error; and (4) m/z matched adduct mass of multiple isobaric species, probable identifications listed. RT: retention time.

m/z	RT	Change in AD	Putative compound(s)	Predicted adduct	ID levels[a]	Notes
129.0661	89	Higher	Glutamine (2 ppm)	$-H_2O + H$	1	–
231.1205	211	Higher	5S,6S-epoxy-15R-hydroxy-ETE-(+Na, 0 ppm)	–	3	–
246.9550	127	Higher	Numerous database matches	$-H_2O + H$	–	Contains halogen (Cl and/or Br)
334.1410	86	Lower	Piperettine (1 ppm)	+Na	4	–
349.1515	80	Lower	Piperine (1 ppm)	+ACN + Na	4	–
386.8946	61	Higher	1,1-Dichloro-2-(dihydroxy-4'-chlorophenyl)-2-(4'-chlorophenyl)ethylene (9 ppm)	+K	2	Contains halogen (Cl and/or Br)
662.0933	158	Higher	GDP-D-mannuronate (+ACN + H[M + 1], 0ppm); Chaetocin (-2H2O + H[M + 1], 8 ppm); Blighinone (+H[M + 1], 9 ppm)	[M + 1] isotope	4	–
663.4524	36	Higher	Lipid A-disaccharide-1-P(+2H, 2 ppm); Aluminium dodecanoate (+K, 2 ppm)	–	4	–

Metabolites associated with aggregating tau protein in both species

The analysis to determine metabolites associated with p-tau in both humans and *C. elegans* was conducted separately for CSF and plasma. Metabolite annotations from mummichog (Schymanksi level 3 confidence (53)) were then used to test for overlap with unique KEGG ID annotation. We identified four CSF-derived metabolites and five plasma-derived metabolites overlapping with metabolites from the aggregating tau *C. elegans* strain associated with CSF p-tau levels in the same direction (Fig. 1G–J).

Metabolites associated with AD dementia vs. normal controls

Since common thresholds for feature filtering in metabolomics preprocessing pipelines may remove low-abundance exogenous chemicals of interest, we conducted a sensitivity analysis to identify plasma metabolites associated with AD (vs. NC) using a lower threshold for missingness (removal of features missing in > 80% of samples) compared to our original study (>20%) (Table 2). One feature elevated in AD, m/z 386.8946, could not be identified with MS/MS due to low abundance but had a unique match in the METLIN database to 1,1-dichloro-2-(dihydroxy-4"-chlorophenyl)-2-(4"-chlorophenyl)ethylene, a metabolite of DDT. Upon examining the relationship of this putative DDT metabolite with other plasma and CSF metabolomic features and their associated metabolic pathways, we found enrichment in glutathione, nitrogen, inflammatory metabolites, purine, and beta-alanine metabolism (Figure S1, Supplementary Material).

DDT uptake in *C. elegans*

The *C. elegans* cuticle is known to be a barrier against absorption of toxicants (21). The nematode is known to possess CYP 450 enzymes, although their repertoire is not as extensive as in mammals (54). We evaluated if *C. elegans* can absorb and metabolize DDT by measuring the levels of p, p'-DDT, p, p'-DDE, p, p'-DDD, o, p'-DDT, o, p'-DDE, and o, p'-DDD in worms using GC-HRMS. In wildtype worms, exposure to 0.3, 3, and 30 μM DDT led to internal levels of 0.27, 0.49, and 1.3 pg of p, p'-DDT in each worm, respectively (Fig. 2A). All metabolites of p, p'-DDT were also detectable and measured in the transgenic strain. In all strains exposed to 3 μM DDT, the levels of p, p'-DDE were about 5 to 10 times lower than p, p'-DDT.

Effect of DDT exposure on *C. elegans* size and egg laying

Assessment of TOF (length) and extinction (optical density) at 46 to 50 hours postsynchronization (~larval stage 4) revealed that the aggregating strain were smaller and with lower density compared to the nonaggregating and wildtype worms. Exposure to DDT reduced the size and density in all strains assessed (Fig. 2C and D). Measurement at 70 to 72 hours postsynchronization (young adulthood) showed that both tau transgenic strains are smaller ($P < 0.0001$) than wildtype worms, with the aggregating strains more severely affected. There was significant interaction between DDT exposure and strain at both time points . Exposure to DDT reduced the size of all strains in a graded manner, with the aggregating strain exposed to DDT being the smallest (Fig. 2E and F). Consistent with a smaller body size, we found fewer eggs retained within all strains exposed to DDT (Fig. 2B), which was statistically significant within the nonaggregating and aggregating strains. There was no significant interaction observed.

Effect of tau protein and DDT on swim behavior of *C. elegans*

The aggregating strain showed differences in wave initiation rate and travel speed compared to the wildtype worms (Fig. 3A and B). Exposure to DDT in the aggregating strain almost doubled the percentage of time the worms spent curling when swimming (average percentage of time spent curling in aggregating worms + solvent control was 1.13%, and in aggregating worms + DDT: 1.83%, $P < 0.001$, Fig. 3C). The aggregating strain showed a lower activity index (average activity index in nonaggregating strain was 388.6 and in aggregating strain was 286.6, $P < 0.01$; Fig. 3D), and a difference in time spent reversing and brushstroke ($P < 0.05$; Figure S2, Supplementary Material) compared to wildtype worms. Exposure to DDT did not significantly alter any swim behavior in the

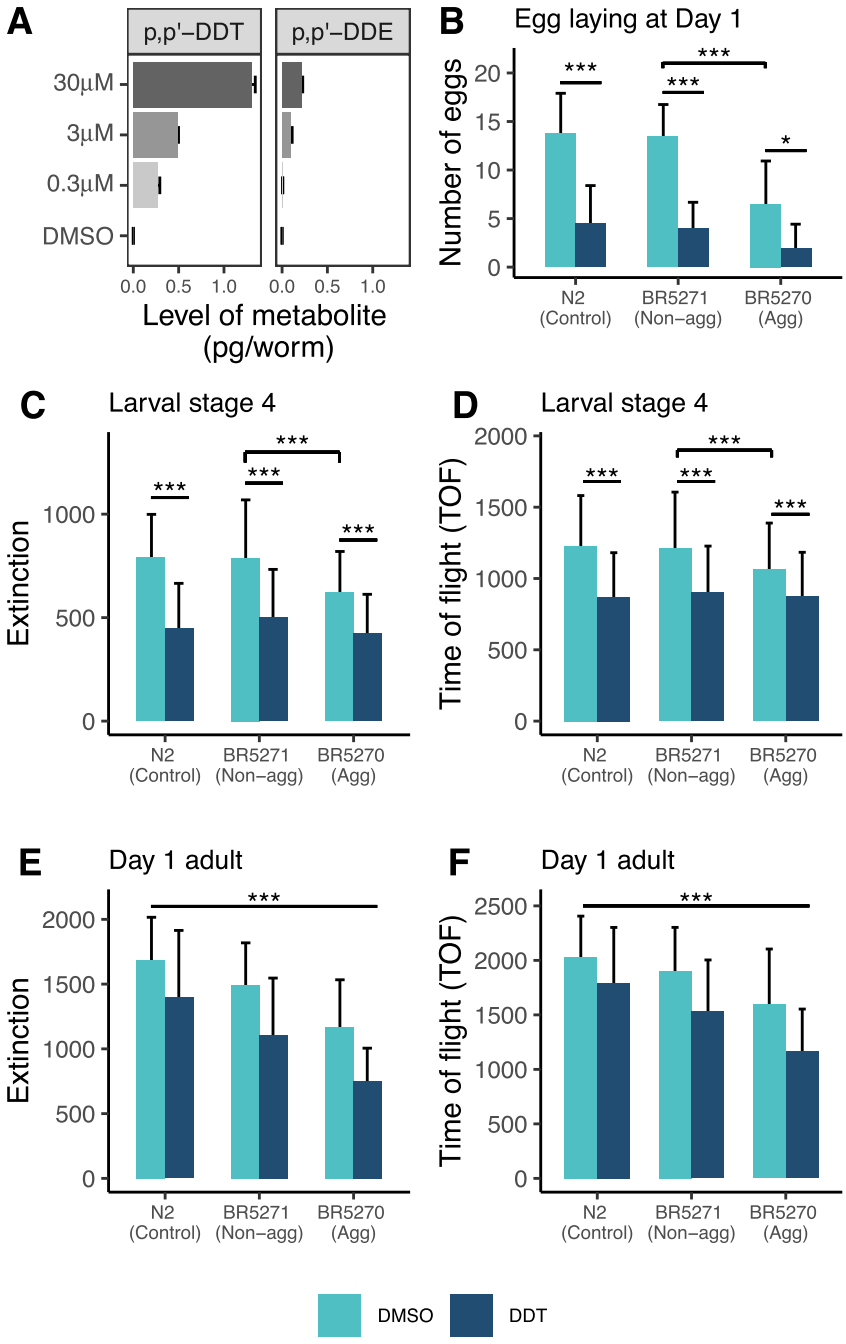

Fig. 2. Uptake and metabolism of DDT and the effect of exposure on growth and egg laying. In wildtype worms, exposure to increasing levels of DDT shows increasing internal levels of p, p'-DDT and its metabolite, p, p'-DDE (A). Wildtype worms exposed to the three doses of DDT were collected in triplicate and the mean level of the parent and its metabolites is plotted with error bars representing the standard deviation. The aggregating strain is smaller in size at larval stage 4 (C) and (D) and in young adulthood (E) and (F) compared to the nonaggregating and wildtype strain. Exposure to DDT restricted the growth of all strains at both stages measured. The bars represent the mean measure and the error bars represent the standard deviation. *** Tukey HSD adjusted $P < 0.0001$.

wildtype or nonaggregating strain. There was a significant interaction between strain and treatment on curling ($P < 0.001$) and wave initiation rate ($P = 0.02$).

Effect of tau and DDT on mitochondrial respiration

Wildtype worms and the nonaggregating strain showed similar oxygen consumption profiles (Fig. 4A). The aggregating strain showed reduced rates of basal, maximal, spare, and nonmitochondrial oxygen consumption rate (OCR) when compared to the nonaggregating strain (Fig. 4B–E). Exposure to 3 μM DDT in the N2 and nonaggregating strain reduced OCR at all four states (Fig. 4A–E). Exposure to DDT in the aggregating strain significantly reduced basal OCR ($P < 0.05$, Fig. 4B). Other measures of respiration were also reduced due to DDT exposure in the aggregating strain however, none were significantly different at $P < 0.05$ (Fig. 4 C–E). There

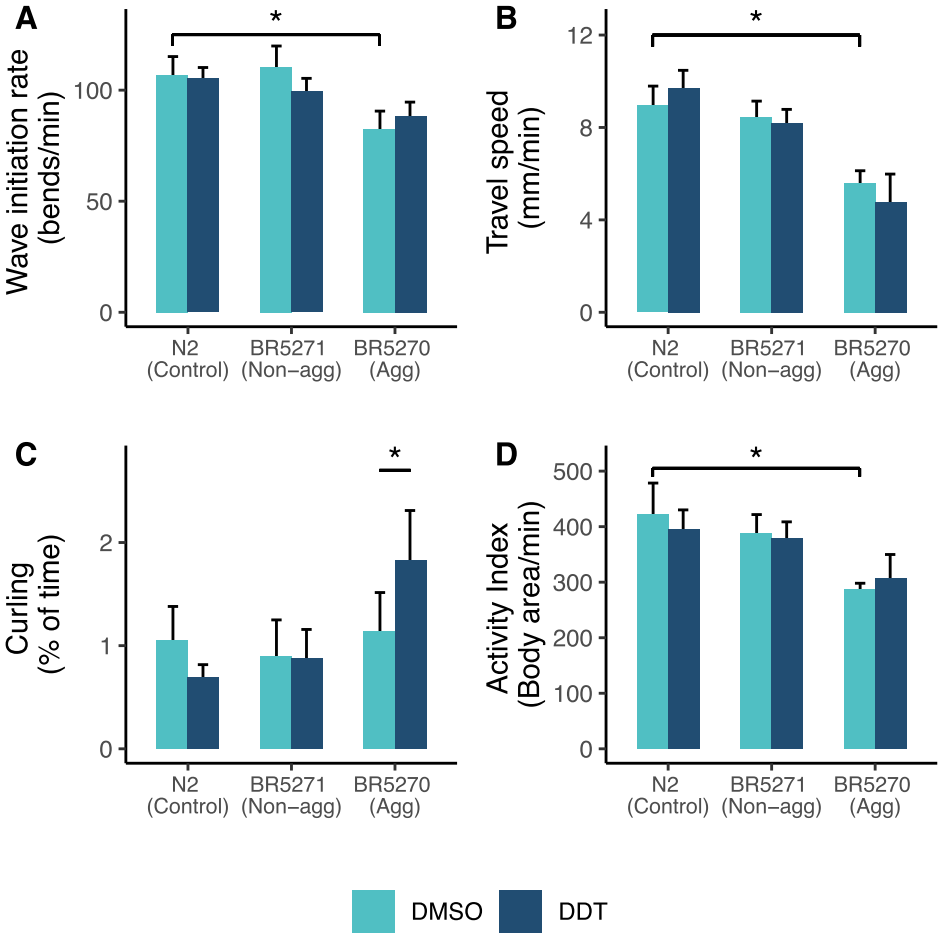

Fig. 3. Aggregating tau and DDT affect swimming behavior. The aggregating strain shows altered wave initiation rate (A) and travel speed (B) compared to the wildtype N2 worm. The aggregating strain exposed to DDT spent more time curling while swimming (C). The overall activity index of the aggregating strain is reduced compared to the wildtype N2 strain (D). Each bar represents the mean measure taken from four-to-five different trials with a total of 50 to 100 worms per group. The error bars represent the standard error of the mean. ∗ Tukey HSD adjusted $P < 0.05$.

was a significant interaction between strain and treatment on all four end points .

Metabolic response to DDT

All strains exposed to DDT showed lower metabolite intensities measured on the HILIC column with positive ionization (Fig. 5A) and the other modes (Figures S3–S5, Supplementary Material). A biplot of principal component (PC) 1 against PC2 shows that the wildtype and nonaggregating strain cluster together while the strains exposed to DDT clustered differently from the unexposed wildtype and nonaggregating strain along PC1 (Fig. 5B). Exposure to DDT altered several amino acids pathways, particularly those that lead to biosynthesis of neurotransmitters (Fig. 5C).

Comparison of metabolic features associated with DDT in human plasma and *C. elegans*

We identified 12 unique metabolites using KEGG IDs obtained from pathway analysis (Fig. 5D; Table S2, Supplementary Material) that were similarly related to DDT/metabolite in worms and human plasma, and five unique metabolites between worms and CSF. We compared the pathways enriched by metabolites associated in *C. elegans*, plasma, and CSF and found enrichment in branched chain amino acid metabolism, tryptophan metabolism, nitrogen metabolism, drug metabolism, and butanoate metabolism (Fig. 5E) in both species.

Effect of DDT exposure on learning

There was no difference in learning determined through the associative learning paradigm among the three strains after adjusting for multiple comparisons; however, the aggregating strain showed a lower learning index compared to the nonaggregating strain. Further, exposure to DDT did not show an effect on learning (Fig. 6A and B). There was no significant interaction between DDT treatment and strain on learning index.

Effect of DDT exposure on survival

The nonaggregating and aggregating strains exhibited a shorter lifespan compared to the wildtype worms (average lifespan in wildtype worms was 24 days, in nonaggregating worms was 19.4 days, and in aggregating worms was 8 days, $P < 0.0001$, Fig. 6C). Exposure to DDT does not alter the lifespan in wildtype or the nonaggregating strain. In the aggregating strain, exposure to DDT slightly rescued the reduction in lifespan in the strain (mean lifes-

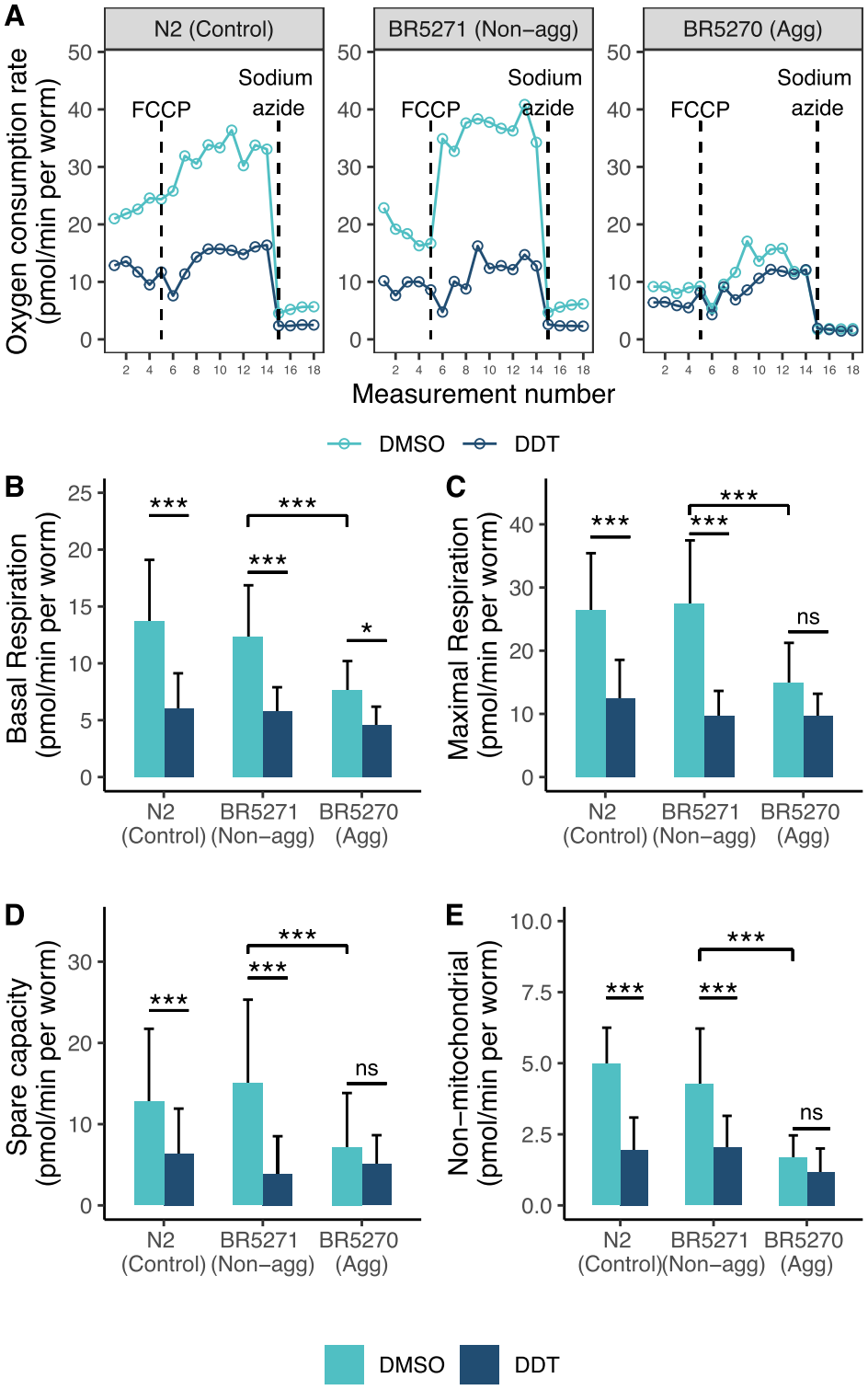

Fig. 4. Aggregating tau and DDT inhibits mitochondrial function. In (A), a representative OCR profile measured using the Seahorse respiratory flux analyzer. The wildtype and nonaggregating strain show a similar OCR however, exposure to DDT reduced the OCR in both strains (A), (B), (C), (D), and (E). The aggregating strain shows a reduced OCR compared to the wildtype and nonaggregating strain (A) and exposure to DDT reduced basal respiration in the aggregating strain (B). Each bar represents the mean respiratory measure made across 3 to 5 experiments with 7 to 12 wells per run with 3 to 30 worms per well. The error bar represents the standard deviation. *** Tukey HSD adjusted $P < 0.0001$, * Tukey HSD adjusted $P < 0.05$, ns: not significant.

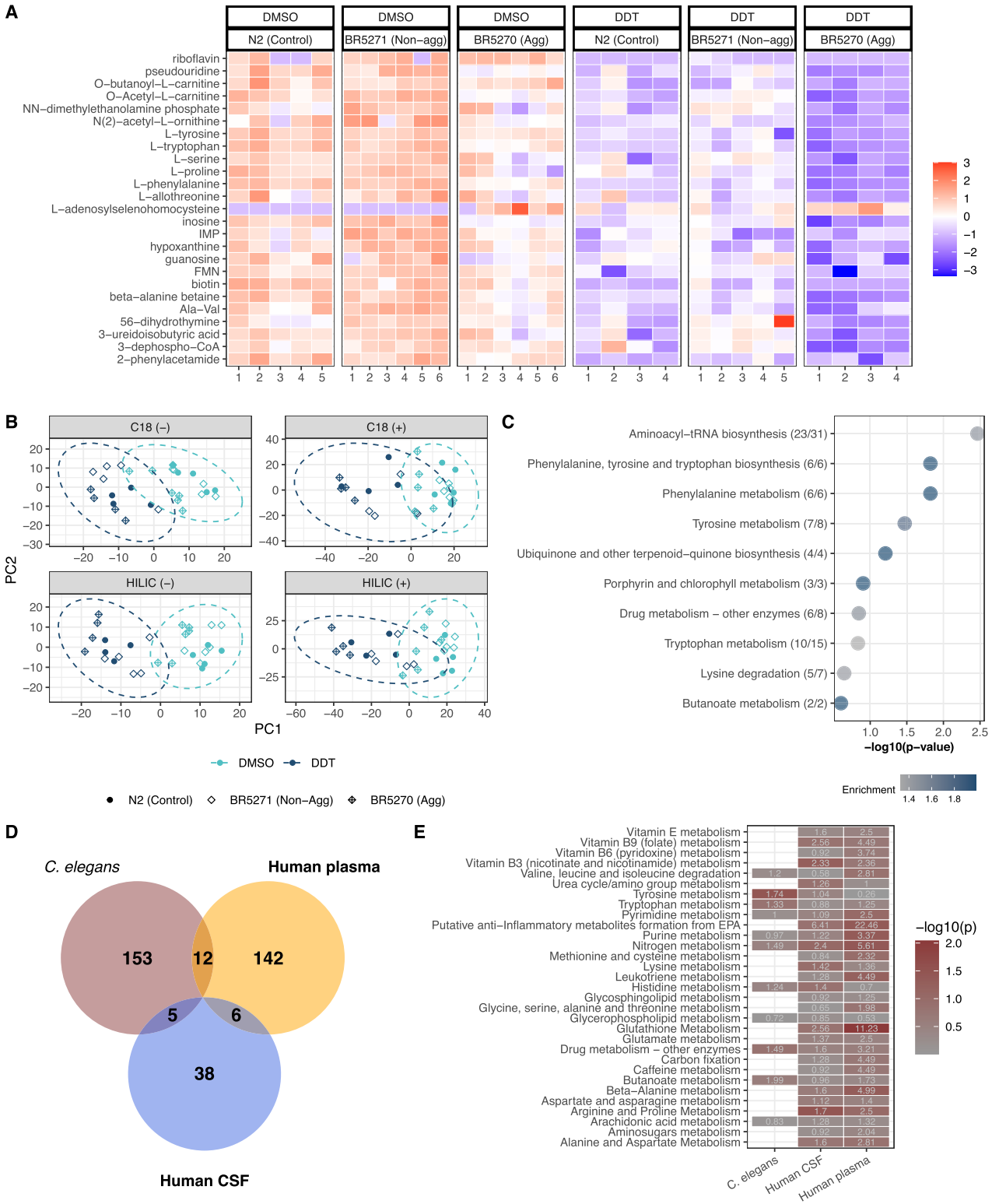

Fig. 5. Metabolomic profile of DDT exposure. In (A), a heatmap of the top 25 metabolites with the smallest *P*-value hierarchically clustered shows that in all strains, DDT decreases metabolite intensity. In (B), a PCA biplot of PC1 plotted against PC2 shows that strains exposed to DDT cluster differently from the wildtype and nonaggregating control strains. The aggregating strain does not cluster with the wildtype and nonaggregating control groups, suggesting variation as a result of aggregating tau protein expression. In (C), the different metabolic pathways enriched by features associated with DDT exposure in the worms. Enrichment is calculated as the ratio between the number of significant hits and the expected number of hits. In (D), the number of features assigned a putative KEGG ID through pathway analysis associated with DDT exposure in worms and with the putative DDT metabolite in human plasma and CSF. In (E), the pathways enriched in both species where the number represents enrichment (ratio between the number of significant hits and the expected number of hits) and the darker red color indicates lower *P*-value. IMP: inosine monophosphate, FMN: flavin mononucleotide, and Ala–Val: alanine–valine dipeptide.

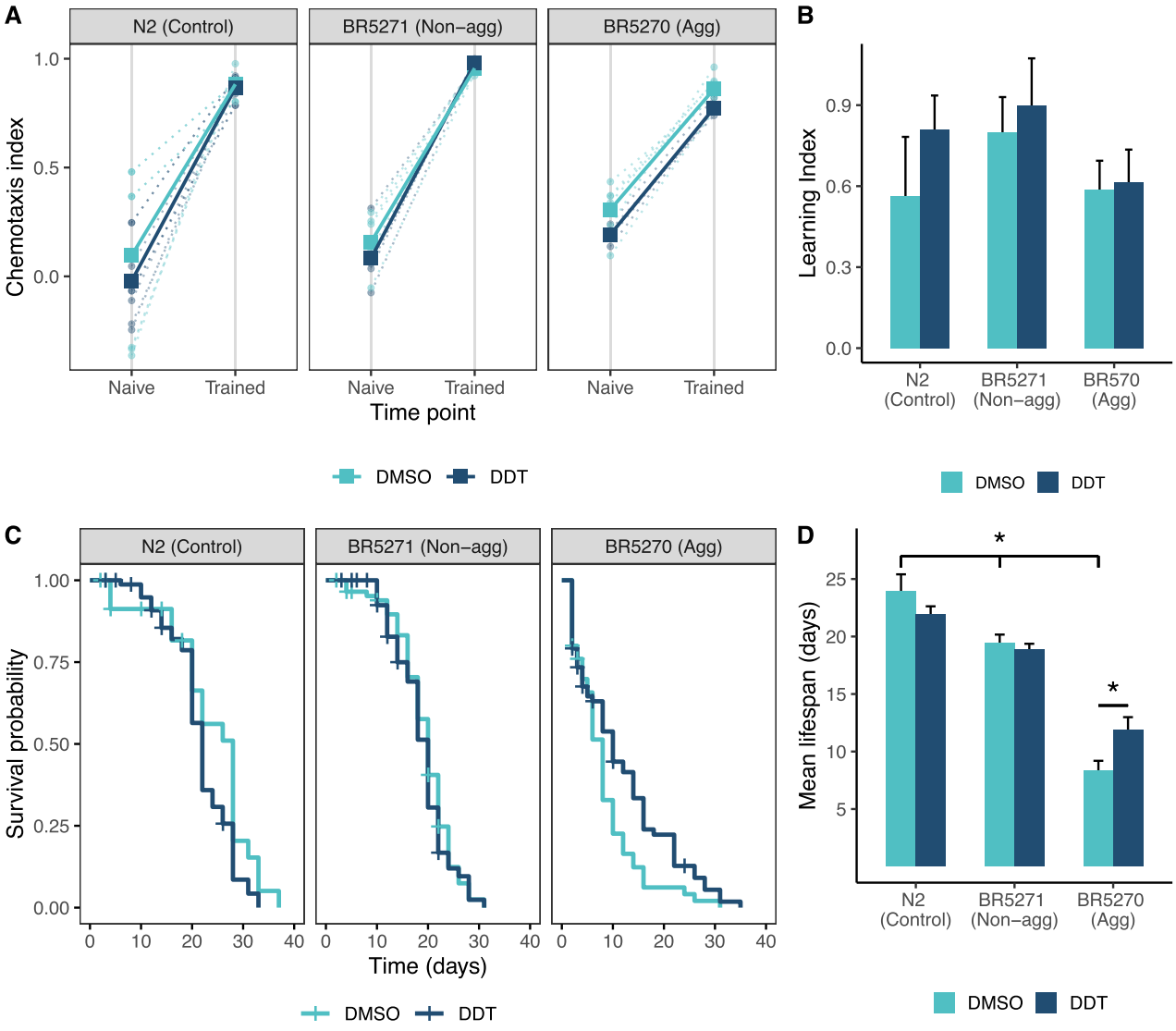

Fig. 6. Associative learning and survival. Associative learning was not affected by exposure to DDT in any of the strains. The aggregating strain did not learn differently from the nonaggregating or wildtype worms. The dotted lines represent the chemotaxis index for each trial with the bold lines representing the mean (A). Each bar represents the learning index (B), calculated as the difference between the trained chemotaxis index, postconditioning, and the naïve chemotaxis index for each trial (A). The error bars represent the standard error of the mean. The nonaggregating and aggregating strain live shorter than wildtype worms. Exposure to DDT did not affect the survival of the wildtype or nonaggregating strains however, exposure to DDT slightly rescued the reduced lifespan in the aggregating strain. The Kaplan–Meier curves (C) are generated by following 60 to 120 worms in each group and the bars (D) represent the mean lifespan in days and the error bars represent the standard deviation. * Tukey HSD adjusted $P < 0.05$.

pan was 11.8 days), however, the lifespan was still shorter than that of the nonaggregating and wildtype strain (Fig. 6C and D). There was a significant interaction between DDT treatment and strain ($P < 0.001$).

Discussion

Model organisms are a useful tool to understand age-related changes in biology and pathology. A number of signaling pathways that act as master regulators of lifespan are conserved in yeast, nematodes, flies, and mammals (55). The use of model systems has uncovered evolutionarily conserved pathways that regulate both longevity and age-related changes in learning and memory (55–61). We used the nematode *C. elegans* to study environmental determinants of aging and cognitive function. The organism's short lifespan (2 to 3 weeks) makes it ideal to study the process of aging and diseases associated with age, such as AD (62–65). In addition, *C. elegans* mitochondria show close structural and functional conservation to mammalian mitochondria (66) and pathways of intermediary metabolism are also highly conserved (67). Thus, we attempted to find similarities in systemic biochemistry associated with aggregating tau protein toxicity, which is a pathological hallmark of AD, in humans and *C. elegans*.

Our group has previously reported plasma metabolites associated with AD in the cohort studied herein (9). The most significant (lowest *P*-value) metabolite associated with CSF p-tau was a metabolite of the drug Rivastigmine, an acetylcholinesterase inhibitor. This was also the top metabolite associated with AD in the previous study. The plasma levels of glutamine were positively associated with levels of CSF p-tau. Metabolomic profiling of the CSF

showed a negative association between CSF levels of p-tau and glutamine, contrary to the direction of the association found in plasma. This could be the result of differential changes in the glutamate/glutamine cycle in the central nervous system and the periphery. The CSF-derived metabolites associated with p-tau levels are related to butanoate metabolism and carnitine shuttle pathways, both of which are associated with mitochondrial function (68, 69).

Using a transgenic strain of *C. elegans* that expresses a mutant form of human tau protein in all neurons, we observed changes in several metabolite peaks that were associated with aggregating tau protein. Pathway analysis using these features revealed changes in metabolic pathways that have previously been associated with neurodegeneration and AD, including the glycerophospholipid pathway, and glyoxylate and dicarboxylate metabolism (70, 71)

The four metabolites associated with p-tau and overlapping between CSF metabolites and worm metabolites were tyrosine, carnitine, cystine, and N, N-dimethylaniline N oxide. While we did not find information on the relationship between N, N-dimethylaniline N oxide and neurodegeneration or AD, all three of the other metabolites have been previously associated with AD. Several studies have reported lower levels of tyrosine measured in the CSF of AD patients (72, 73). An untargeted HRMS-metabolomics analysis of CSF samples from MCI patients showed altered tyrosine metabolism (74). A study of CSF from non-*APOE4* carriers in the early stage of AD reported lower levels of carnitine in the CSF (75). Another study of CSF from AD patients found lower levels of free carnitine but increased levels of acylcarnitine suggesting impaired energy production through anaplerotic pathways (76). We detected decreased levels of cystine in plasma, CSF, and worms. Cystine is the dimer form of cysteine, a sulfur containing amino acid that functions to reduce redox stress. Several studies have reported increased levels of cysteine in the brain, plasma, and CSF of AD patients (77–79). This could be a result of increased conversion of cystine to cysteine to ameliorate oxidative stress.

Apart from cystine, the other metabolites associated with p-tau found to be overlapping between plasma and worms were lipoamide, diethylthiophosphoric acid, 11,12-dihydroxy-5Z,8Z,14Z-eicosatrienoic acid (11,12-DHET), and N-acetyl lysine. Lipoamide is the amide form of lipoic acid, which is a naturally occurring disulfide compound that functions as a cofactor for mitochondrial bioenergetic enzymes. It has been proposed as a novel treatment for AD owing to the many functions it performs (80). Lipoic acid can increase acetylcholine production (81) and glucose uptake (80) and it is reported to improve peripheral insulin resistance and impaired glucose metabolism (82–84). Diethylthiophosphoric acid is a part of the aminobenzoate degradation pathway. Derivatives of aminobenzoic acid may have potential as drugs to inhibit acetylcholinesterase, thereby ameliorating the acetylcholine deficit present in AD (85). 11,12-DHET derives from oxidation of arachidonic acid, a well-known precursor activated during inflammatory response. A study using strains of mice expressing Aβ and tau in the brain found increased levels of several eicosanoids in the brain and in plasma of these mice (86). In both human plasma and worms we found higher levels of DHET, in line with previous findings. Finally, altered lysine metabolism has been previously reported in cases of MCI compared to cognitively normal individuals (79) and lysine supplementation has been proposed as a treatment strategy for AD (87).

Neither the human nor *C. elegans* metabolome is fully curated, and nontargeted metabolomics data includes many dietary, microbiome, and environmental chemicals in addition to those associated with endogenous metabolic pathways as presented here. Although the results from this cross-species analysis should be interpreted with caution, the concordance between several metabolites that have been previously associated with AD provides support for using *C. elegans* as a model to study biochemical changes associated with AD-related pathology. Further, the disruptions in evolutionarily conserved pathways that are associated with AD-related related pathology offer great power for mechanistic interpretation. Correlation between metabolites observed across species could provide a means to identify overlapping central networks and interacting subnetworks associated with AD-related pathology (88). In the future, we plan to use mutant strains and appropriate exposures to determine the role of these metabolites in the aggregating tau protein related toxicity in *C. elegans*.

Untargeted HRMS-metabolomics approaches allow us to study the effects of the exposome on human health (89). However, in untargeted HRMS-metabolomics analyses, the abundance of exogenously derived parent compounds and their metabolites tend to be orders of magnitude lower than endogenous chemicals (90) and may not be present in all study participants. Thus, statistical approaches and thresholds need to be adjusted to account for this lower abundance and prevalence of exogenous chemicals in population studies. Therefore, we conducted a sensitivity analysis by applying a lower threshold for feature filtering in our previous analysis of plasma-derived features associated with AD. The analysis found higher levels of a halogenated metabolite in the plasma of AD patients, which was putatively identified as a derivative of the persistent pesticide DDT (Table 2).

We assayed the level of DDT in the transgenic worms exposed to the pesticides using a targeted GC-HRMS assay, which detected and measured several metabolites of the pesticide, suggesting that DDT is not only absorbed but also biotransformed in the nematode, supporting the use of this model to study the toxic effects of DDT. Previously, Mahmood (91) found that exposure to 1 μg/mL of DDT (~2.8 μM) had a mild inhibitory effect on pharyngeal pumping, while this dose had no effect on brood size. A survey of serum samples analyzed for levels of p, p'-DDT conducted by NHANES showed a wide range of the pesticide in the blood of the American population, and levels of p, p'-DDT measured increased with increasing age. Among those aged 12 to 19 years in the survey, the geometric mean of lipid adjusted serum p, p'-DDT level was less than 5 ng/g lipid (CDC 2020). Assuming the wet mass of a single worm is 1 μg (92), exposure to 3 μM DDT using our paradigm resulted in a mean level of ~0.5 ng/g wet weight of *C. elegans*. Thus, we exposed the wildtype, aggregating, and nonaggregating strains to 3 μM DDT during development and measured the effect of exposure on various outcomes: swim behavior, respiration, growth, global metabolomic profiles, learning, and lifespan. These phenotypes were tested based on previous studies that have reported changes in AD and tau protein toxicity. First, given that cognitive impairment is a salient feature of AD, we tested the effect of exposure on associative memory. Second, studies have reported altered mitochondrial function and energy metabolism in the brain of AD patients (93–95), some report these alterations before Aβ aggregate formation (96, 97). Indeed, animal studies have also reported that oxidative stress, mitochondrial dysfunction, and metabolic alterations are early events in AD pathogenesis (98, 99). In a PET and MRI imaging study, brain glucose and acetoacetate metabolism were altered in patients with AD (100). Proteomic analyses have reported that several glycolysis and mitochondrial TCA cycle enzymes are oxidized in the AD brain (101). Non-neuronal cells derived from AD patients also showed altered energy metabolism (102–105), suggesting that these changes in

metabolism are systemic and not restricted to the central nervous system. Based on these findings, we tested whether exposure to DDT and tau protein toxicity affects growth, swim characteristics associated with mitochondrial toxicity, global metabolism, and lifespan. Finally, mitochondrial dysfunction has been identified as an important factor involved in the early pathology of AD. Mitochondrial dynamics and transport, which is critical for proper energy production and synaptic function, has been reported to be altered in AD (106). Metabolic pathways associated with oxidative phosphorylation and energy production like nicotinamide adenine dinucleotide metabolism and the citric acid cycle were found to be reduced (107). Indeed, studies have reported a "Warburg-like effect" in mild cases of AD, whereby neurons prefer to produce energy through glycolysis and mitochondria appear quiescent, likely due to Aβ related toxicity (108). Therefore, we tested the effect of exposure on mitochondrial function.

Similar to previous findings (29), we observed that the aggregating strain travels slower than the wildtype worms. The aggregating strain also showed a reduced wave initiation rate, which is akin to a swimming stroke rate (36), compared with the nonaggregating and wildtype strain. Additionally, the aggregating strain had a lower overall activity index compared with the nonaggregating and wildtype strain. Exposure to DDT significantly increased the amount of time the aggregating strain spent curling. The curling phenotype has been used to screen for motility defects in worms. A recent screen for curling identified the *bcat-1* gene to be associated with a Parkinson's-like phenotype and knockdown of the gene transcript showed altered mitochondrial function (45). The curling phenotype has also been used to ascertain dopaminergic toxicity due to the complex I inhibition by MPP^+ (109, 110).

We observed that the aggregating strain has severely impaired mitochondrial respiration, with diminished basal and maximal respiration compared with the nonaggregating strain. Several in vitro and in vivo studies have shown that aggregating tau protein can inhibit complex I and V of the mitochondria (111–113). Tau protein can alter the mitochondrial membrane potential, cause activation of the apoptotic-related caspase-9, and impede energy production (113, 114). Furthermore, disintegration of tau protein can lead to disturbed transport of mitochondria across microtubules and mitochondrial fission–fusion dynamics (29, 115).

Exposure to DDT in the wildtype and nonaggregating strain severely impaired mitochondrial respiration at baseline and in the uncoupled state (FCCP). Several in vitro and in vivo studies have reported an inhibitory effect of DDT on mitochondrial function and ATP production, but none have reported this in *C. elegans*. DDT is known to inhibit complex II, III, and V of the electron transport chain and it depresses the mitochondrial membrane potential (116, 117). In rats, exposure to DDT reduced the number of mitochondria measured in the liver and altered fatty acid metabolism (118), an effect that would be consistent with the overall decrease in OCR under all states measured. We note that this overall decrease in oxidative phosphorylation activity is also unlikely to be attributable to decreased motility since exposure to DDT did not affect the swimming behavior of wildtype worms, reinforcing the interpretation that DDT may directly affect either mitochondrial content and/or respiratory chain activity.

We found that the aggregating strain was smaller in size at larval stage 4 and at day 1 of adulthood compared to the nonaggregating strain. When exposed to DDT, there was no difference in size between the aggregating and nonaggregating strains at larval stage 4; however, on day 1 of adulthood, DDT reduced the size of the aggregating strain more than in the nonaggregating strain. Similarly, we found that DDT-exposed worms contained fewer eggs at day 1 of adulthood. This is consistent with a DDT-induced developmental delay, resulting in a smaller size at each developmental time point measured and slower time to reproductive maturity and egg formation. DDT exposure has been shown to cause developmental delay in babies exposed in utero, with those exposed to the highest levels of DDT showing the greatest deficits in two measures of neurodevelopment, including the Bayley Psychomotor Development Index and the Mental Development Index (119). Another possibility to explain this egg deficit could include reproductive toxicity. *Caenorhabditis elegans* exposed to endosulfan, another organochlorine pesticide, showed reduced fecundity and, of the eggs that were laid, reduced hatchability. The same paper also showed germ cell line apoptosis in both endosulfan and DDT exposed worms (120). Lastly, and most closely in line with possible neurologic deficits, acetylcholine has been shown to inhibit egg-laying behavior (121). Therefore, deficits in cholinergic signaling would cause increased egg laying and, therefore, less egg-retention in the body. However, further studies would be needed in order to delineate the exact mechanism underlying reduced egg number in DDT exposed worms.

HRMS-metabolomics identified several metabolites that were altered in worms following DDT exposure. Levels of several amino acids that are precursors to neurotransmitters were altered. Levels of uric acid were ~2-fold higher in worms exposed to DDT. Uric acid is the end product of purine metabolism and has antioxidant properties since it can scavenge free radicals and prevent lipid peroxidation (122). High levels of uric acid have been reported to induce stress response pathways in *C. elegans* by increasing levels of the DAF-16/FOXO and SKN-1/NRF-2 transcripts (123). Levels of adenosylselenohomocysteine were also found to be increased in all strains exposed to DDT and in the aggregating strain (Fig. 5A). Thioredoxin reductase-1 (TrxR-1) is the only selenium containing protein in *C. elegans* (124). An elevated seleno-metabolite suggests increased levels of TrxR-1 in response to oxidative stress induced by DDT exposure and tau protein aggregation.

Comparison of metabolites associated with DDT and its metabolites in worms and human plasma and CSF revealed similar changes in amino acids and metabolites of the inflammatory pathways (Table S2, Supplementary Material). The overlapping metabolic pathways indicate changes in drug metabolism pathways, as expected, and additionally, changes in metabolism of precursors of neurotransmitters, butanoate metabolism, and pyrimidine metabolism, which have been previously reported to be associated with exposure to DDT metabolites and organochlorine pesticides (125, 126). The concordance between the species further strengthens the use of *C. elegans* as a model relevant to studying the metabolic effect of exposure to toxicants on human health.

The aggregating strain did not show any difference in their ability to learn following an associative training paradigm, compared to the nonaggregating or wildtype strain. These findings are similar to those made by Wang and colleagues (127). Exposure to DDT did not affect this ability to learn in either strain using the associative learning assay.

We found that the nonaggregating and aggregating strains have a reduced lifespan compared to wildtype worms, replicating previous findings (127). The proteotoxicity and reduced respiratory rate in the aggregating strain could explain this observation (128). Interestingly, exposure to DDT did not change the mean lifespan in wildtype or nonaggregating worms but it slightly increased the mean lifespan of the aggregating strain. This finding is surprising but given that the exposure occurred developmentally, it hints to the activation of mitohormetic pathways, which could turn

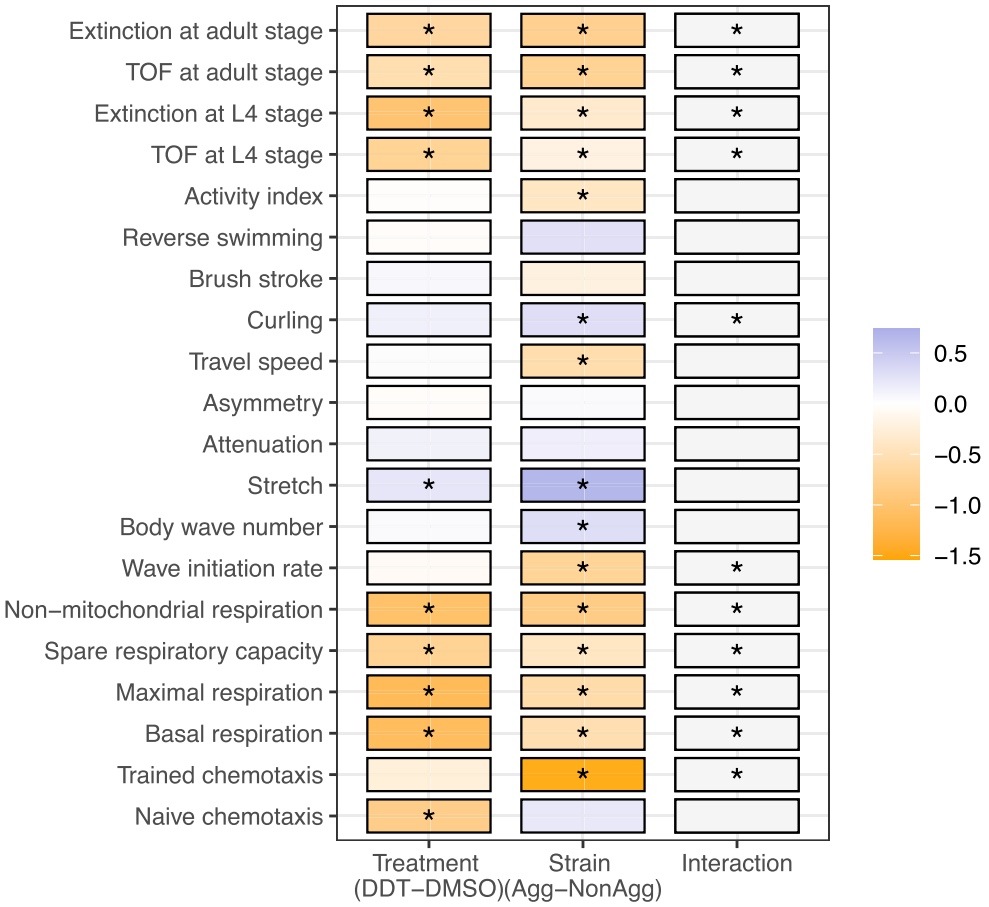

Fig. 7. A summary of the results. This plot summarizes results from two-way ANOVAs with asterisks indicating significant interaction between treatment and strain for each outcome and color indicating the scaled direction and strength of the association between treatment or strain with each outcome.

on lifespan extension pathways (129), like the mitochondrial unfolded protein response (UPR^{mt}) pathway. However, the extension in lifespan was not large enough to be as much or more than the lifespan of the nonaggregating or wildtype strain. It is also possible that, while mitochondrial inhibition by aggregating tau protein alone does not induce the UPR^{mt} pathways, the mitochondrial stress induced by DDT during development produces an antagonistic effect which induces stress response pathways (130).

The results from the different end points indicate that DDT is toxic independent of strains; and behaviors influenced by strain, like wave initiation rate, curling, travel speed, and activity index, are more meaningful endpoints that should be tested for interaction (Fig. 7).

While we present evidence that supports the use of *C. elegans* as a model to study whether DDT can exacerbate tau protein toxicity, our study has limitations. In insects and mammals, DDT inhibits voltage-gated sodium channel inactivation and stabilizes the open state of sodium channels, causing prolonged channel opening (131, 132). The *C. elegans* genome does not encode for voltage-gated sodium channels (133), thus DDT does not produce neurotoxicity through this mechanism in the nematode. Thus, we were unable to measure any interaction tau protein aggregation may have with altered neuronal excitability elicited by DDT in mammalian neurons. However, DDT is known to also target mammalian nuclear hormone receptors(134–136), many of which have orthologues in *C. elegans* (137), providing plausible targets of DDT in worms responsible for the effects observed in this study, like the nuclear hormone receptor-85 that is known to mediate egg-laying behavior (137). In the transgenic model we chose, we were unable to control the level of tau protein aggregates expressed in the neurons. It is possible that the severe tau protein aggregation toxicity obscured effects of DDT exposure and its proteotoxic effects. The interactions between the two insults may become more apparent when lower levels of the aggregates are expressed.

Despite these limitations, we provide evidence that support the use of *C. elegans* as a model to study gene–environment interactions. We provide evidence that DDT is taken up and biotransformed by *C. elegans*. In wildtype worms, DDT restricts growth, as measured by size, and reduces mitochondrial respiration. DDT produces major changes in global metabolism, including pathways related to neurotransmitter precursors and other amino acid metabolism. In transgenic worms that express an aggregating form of human tau protein in all neurons, DDT restricts growth even further and reduces the basal respiration rate. Aggregating tau worms exposed to DDT spend more time curling when swimming, a known mitochondrial toxicity phenotype. Further, DDT exposure affects the metabolism of several amino acids that are precursors to biosynthesis of neurotransmitter. Our data suggest that exposure to DDT likely exacerbates the mitochondrial inhibitory effects of aggregating tau protein in *C. elegans*. Additionally, the concordance between several metabolites that have been previously associated with AD provides validity to using *C. elegans* as a model to study biochemical changes associated with AD-

related pathology. In the future, using transgenic *C. elegans* strains, we will perform systematic analyses of the environmental drivers of AD that can lead to interventional strategies aimed at preventing or treating the disease.

Supplementary material

Supplementary material is available at *PNAS Nexus* online.

Funding

G.W.M is supported by the NIH grants RF1AG066107, R01AG067501, U2C ES030163, R01ES023839, and UL1-TR00187; F.L.A. and M.L.B. are supported by the NIEHS grant T32ES007732; D.I.W. is supported by the NIEHS grant U2C ES030859; and K.E.M. is supported by the NEIHS grant T32ES007272.

Author Contributions

V.K. designed the research, performed the research, analyzed the data, and wrote the paper; M.N. designed the research and analyzed the data; J.B. designed the research and performed the research; F.L. performed the research; F.A. performed the research and wrote the paper; M.B. performed the research; K.M. performed the research and wrote the paper; A.S. performed the research; Z.C.F. performed the research; K.P. designed the research and wrote the paper; M.P. designed the research and wrote the paper; D.W. designed the research, analyzed the data, and wrote the paper; W.H. designed the research and wrote the paper; D.J. designed the research and wrote the paper; and G.M. designed the research and wrote the paper.

Data availability

The patient-related metabolomics data will be made available on metabolomics workbench. All data and code related to DDT exposure in *C. elegans* is available through a repository on VK's GitHub and can accessed through zenodo, DOI: 10.5281/zenodo.6342389.

References

1. Matthews KA, *et al.* 2019. Racial and ethnic estimates of Alzheimer's disease and related dementias in the United States (2015–2060) in adults aged ≥65 years. Alzheimer's Dementia J Alzheimer's Assoc 15:17–24.
2. Van Cauwenberghe C, Van Broeckhoven C, Sleegers K. 2016. The genetic landscape of Alzheimer disease: clinical implications and perspectives. Genet Med 18:421–430.
3. de la Monte SM, Wands JR. 2008. Alzheimer's disease is type 3 diabetes-evidence reviewed. J Diabetes Sci Technol 2:1101–1113.
4. Bischof GN, Park DC. 2015. Obesity and aging: consequences for cognition, brain structure, and brain function. Psychosom Med 77:697–709.
5. Ossenkoppele R, *et al.* 2015. Tau, amyloid, and hypometabolism in a patient with posterior cortical atrophy. Ann Neurol 77:338–342.
6. Ossenkoppele R, *et al.* 2016. Tau PET patterns mirror clinical and neuroanatomical variability in Alzheimer's disease. Brain 139:1551–1567.
7. Pérez MJ, Jara C, Quintanilla RA. 2018. Contribution of Tau pathology to mitochondrial impairment in neurodegeneration. Front Neurosci 12:441.
8. Nichols E, *et al.* 2019. Global, regional, and national burden of Alzheimer's disease and other dementias, 1990–2016: a systematic analysis for the Global Burden of Disease Study 2016. Lancet Neurol 18:88–106.
9. Niedzwiecki MM, *et al.* 2020. High-resolution metabolomic profiling of Alzheimer's disease in plasma. Ann Clin Transl Neurol 7:36–45.
10. Vardarajan B, *et al.* 2020. Differences in plasma metabolites related to Alzheimer's disease, APOE $\varepsilon 4$ status, and ethnicity. Alzheimer's Dementia Transl Res Clin Intervent 6:e12025.
11. DeKosky ST, Gandy S. 2014. Environmental exposures and the risk for Alzheimer disease: can we identify the smoking guns?. JAMA Neurol 71:273–275.
12. Richardson JR, *et al.* 2014. Elevated serum pesticide levels and risk for Alzheimer disease. JAMA Neurol 71:284–290.
13. Turusov V, Rakitsky V, Tomatis L. 2002. Dichlorodiphenyltrichloroethane (DDT): ubiquity, persistence, and risks. Environ Health Perspect 110:125–128.
14. Centers for Disease Control and Prevention. 2020. National report on human exposure to environmental chemicals. Atlanta, GA: Centers for Disease Control and Prevention. 2020 Nov 27.
15. Needham LL, *et al.* 2011. Partition of environmental chemicals between maternal and fetal blood and tissues. Environ Sci Technol 45:1121–1126.
16. van den Berg H, Manuweera G, Konradsen F. 2017. Global trends in the production and use of DDT for control of malaria and other vector-borne diseases. Malar J 16:401.
17. Wania F, Mackay D. 1996. Peer reviewed: tracking the distribution of persistent organic pollutants. Environ Sci Technol 30:390A–396A.
18. Boyd WA, *et al.* 2016. Developmental effects of the ToxCast™ phase I and phase II chemicals in *Caenorhabditis elegans* and corresponding responses in zebrafish, rats, and rabbits. Environ Health Perspect 124:586–593.
19. Cole RD, Anderson GL, Williams PL. 2004. The nematode *Caenorhabditis elegans* as a model of organophosphate-induced mammalian neurotoxicity. Toxicol Appl Pharmacol 194:248–256.
20. Harlow PH, *et al.* 2016. The nematode *Caenorhabditis elegans* as a tool to predict chemical activity on mammalian development and identify mechanisms influencing toxicological outcome. Sci Rep 6:22965.
21. Hunt PR. 2017. The *C. elegans* model in toxicity testing. J Appl Toxicol 37:50–59.
22. Hunt PR, Olejnik N, Sprando RL. 2012. Toxicity ranking of heavy metals with screening method using adult *Caenorhabditis elegans* and propidium iodide replicates toxicity ranking in rat. Food Chem Toxicol 50:3280–3290.
23. Middendorf PJ, Dusenbery DB. 1993. Fluoroacetic acid is a potent and specific inhibitor of reproduction in the nematode *Caenorhabditis elegans*. J Nematol 25:573–577.
24. Williams PL, Dusenbery DB. 1988. Using the nematode *Caenorhabditis elegans* to predict mammalian acute lethality to metallic salts. Toxicol Ind Health 4:469–478.
25. C. elegans Sequencing Consortium. 1998. Genome sequence of the nematode *C. elegans*: a platform for investigating biology. Science 282:2012–2018.
26. Kaletta T, Hengartner MO. 2006. Finding function in novel targets: *C. elegans* as a model organism. Nat Rev Drug Discov 5:387–399.

27. Brenner S. 1974. The genetics of *Caenorhabditis elegans*. Genetics 77:71–94.
28. Corsi AK, Wightman B, Chalfie M. 2015. A transparent window into biology: a primer on *Caenorhabditis elegans*. The C. elegans Research Community, WormBook, 1–31. http://www.wormbook.org.
29. Fatouros C, *et al.* 2012. Inhibition of tau aggregation in a novel *Caenorhabditis elegans* model of tauopathy mitigates proteotoxicity. Hum Mol Genet 21:3587–3603.
30. Irwin D, *et al.* 2017. Ante mortem CSF tau levels correlate with post mortem tau pathology in FTLD. Ann Neurol 82:247–258.
31. Albert MS, *et al.* 2011. The diagnosis of mild cognitive impairment due to Alzheimer's disease: recommendations from the National Institute on Aging-Alzheimer's Association workgroups on diagnostic guidelines for Alzheimer's disease. Alzheimers Dement 7:270–279.
32. McKhann GM, *et al.* 2011. The diagnosis of dementia due to Alzheimer's disease: recommendations from the National Institute on Aging-Alzheimer's Association workgroups on diagnostic guidelines for Alzheimer's disease. Alzheimers Dement 7:263–269.
33. Hu WT, *et al.* 2015. CSF beta-amyloid 1-42 – what are we measuring in Alzheimer's disease?. Ann Clin Transl Neurol 2:131–139.
34. Howell JC, *et al.* 2017. Race modifies the relationship between cognition and Alzheimer's disease cerebrospinal fluid biomarkers. Alzheimers Res Ther 9:88.
35. Hunt PR, *et al.* 2011. Extension of lifespan in *C. elegans* by naphthoquinones that act through stress hormesis mechanisms. PLoS ONE 6:e21922.
36. Restif C, *et al.* 2014. CeleST: computer vision software for quantitative analysis of *C. elegans* swim behavior reveals novel features of locomotion. PLoS Comput Biol 10:e1003702.
37. Koopman M, *et al.* 2016. A screening-based platform for the assessment of cellular respiration in *Caenorhabditis elegans*. Nat Protoc 11:1798–1816.
38. Kauffman A, *et al.* 2011. *C. elegans* positive butanonelearning, short-term, and long-term associative memory assays. J Vis Exp 39:2490. DOI:10.3791/2490.
39. vonderEmbse AN, Elmore SE, Jackson KB. *et al.* 2021. Developmental exposure to DDT or DDE alters sympathetic innervation of brown adipose in adult female mice. Environ Health 20: 37, doi:10.1186/s12940-021-00721-2.
40. Manz KE, *et al.* 2021. Targeted and nontargeted detection and characterization of trace organic chemicals in human serum and plasma using QuEChERS extraction. Toxicol Sci 185: 77–88..
41. Go Y-M, *et al.* 2015. Reference standardization for mass spectrometry and high-resolution metabolomics applications to exposome research. Toxicol Sci 148:531–543.
42. Park YH, *et al.* 2012. High-performance metabolic profiling of plasma from seven mammalian species for simultaneous environmental chemical surveillance and bioeffect monitoring. Toxicology 295:47–55.
43. Soltow QA, *et al.* 2013. High-performance metabolic profiling with dual chromatography-Fourier-transform mass spectrometry (DC-FTMS) for study of the exposome. Metabolomics 9:S132–S143.
44. Bradner JM, *et al.* 2021. Genetic or toxicant-induced disruption of vesicular monoamine storage and global metabolic profiling in *Caenorhabditis elegans*. Toxicol Sci 180:313–324. DOI: 10.1093/toxsci/kfab011. 2021 Mar 8.
45. Mor DE, *et al.* 2020. Metformin rescues Parkinson's disease phenotypes caused by hyperactive mitochondria. Proc Natl Acad Sci 17:26438–26447. DOI:10.1073/pnas.2009838117 2020 Oct 6.
46. Liu KH, *et al.* 2020. Reference standardization for quantification and harmonization of large-scale metabolomics. Anal Chem 92:8836–8844.
47. Yu T, Park Y, Johnson JM, Jones DP. 2009. apLCMS—adaptive processing of high-resolution LC/MS data. Bioinformatics 25:1930–1936.
48. Uppal K, *et al.* 2013. xMSanalyzer: automated pipeline for improved feature detection and downstream analysis of large-scale, non-targeted metabolomics data. BMC Bioinf 14:15.
49. Leek JT, Johnson WE, Parker HS, Jaffe AE, Storey JD. 2012. The sva package for removing batch effects and other unwanted variation in high-throughput experiments. Bioinformatics 28:882–883.
50. Li S, *et al.* 2013. Predicting network activity from high throughput metabolomics. PLoS Comput Biol 9:e1003123.
51. Pang Z, Chong J, Li S, Xia J. 2020. MetaboAnalystR 3.0: toward an optimized workflow for global metabolomics. Metabolites 10:186.
52. Chong J, *et al.* 2018. MetaboAnalyst 4.0: towards more transparent and integrative metabolomics analysis. Nucleic Acids Res 46:W486–W494.
53. Schymanski EL, *et al.* 2014. Identifying small molecules via high resolution mass spectrometry: communicating confidence. Environ Sci Technol 48:2097–2098.
54. Harlow PH, Perry SJ, Stevens AJ, Flemming AJ. 2018. Comparative metabolism of xenobiotic chemicals by cytochrome P450s in the nematode *Caenorhabditis elegans*. Sci Rep 8:13333.
55. Bishop NA, Lu T, Yankner BA. 2010. Neural mechanisms of ageing and cognitive decline. Nature 464:529–535.
56. Friedman DB, Johnson TE. 1988. A mutation in the age-1 gene in *Caenorhabditis elegans* lengthens life and reduces hermaphrodite fertility. Genetics 118:75–86.
57. Grotewiel MS, Martin I, Bhandari P, Cook-Wiens E. 2005. Functional senescence in *Drosophila melanogaster*. Ageing Res Rev 4:372–397.
58. Kauffman AL, Ashraf JM, Corces-Zimmerman MR, Landis JN, Murphy CT, 2010. Insulin signaling and dietary restriction differentially influence the decline of learning and memory with age. PLoS Biol 8:e1000372.
59. Kenyon C, Chang J, Gensch E, Rudner A, Tabtiang R. 1993. A *C. elegans* mutant that lives twice as long as wild type. Nature 366:461–464.
60. Klass MR, 1977. Aging in the nematode *Caenorhabditis elegans*: major biological and environmental factors influencing life span. Mech Ageing Dev 6:413–429.
61. Silva AJ, Kogan JH, Frankland PW, Kida S. 1998. Creb and memory. Annu Rev Neurosci 21:127–148.
62. Ardiel EL, Rankin CH. 2010. An elegant mind: learning and memory in *Caenorhabditis elegans*. Learn Mem 17:191–201.
63. Arey RN, Murphy CT. 2017. Conserved regulators of cognitive aging: from worms to humans. Behav Brain Res 322:299–310.
64. Jonsson T, *et al.* 2013. Variant of TREM2 associated with the risk of Alzheimer's disease. N Engl J Med 368:107–116.
65. Link CD. 2006. *C. elegans* models of age-associated neurodegenerative diseases: lessons from transgenic worm models of Alzheimer's disease. Exp Gerontol 41:1007–1013.
66. Murfitt RR, Vogel K, Sanadi DR. 1976. Characterization of the mitochondria of the free-living nematode, *Caenorhabditis elegans*. Comp Biochem Physiol Part B Comp Biochem 53:423–430.

67. O'Riordan VB, Burnell AM. 1990. Intermediary metabolism in the dauer larva of the nematode *Caenorhabditis elegans*—II. the glyoxylate cycle and fatty-acid oxidation. Compar Biochem Physiol Part B Comp Biochem 95:125–130.
68. Pettegrew JW, Levine J, McClure RJ. 2000. Acetyl- L -carnitine physical-chemical, metabolic, and therapeutic properties: relevance for its mode of action in Alzheimer's disease and geriatric depression. Mol Psychiatry 5:616–632.
69. Rose S, *et al.* 2018. Butyrate enhances mitochondrial function during oxidative stress in cell lines from boys with autism. Transl Psychiatry 8:1–17.
70. Frisardi V, Panza F, Seripa D, Farooqui T, Farooqui AA. 2011. Glycerophospholipids and glycerophospholipid-derived lipid mediators: a complex meshwork in Alzheimer's disease pathology. Prog Lipid Res 50:313–330.
71. Yan X, Hu Y, Wang B, Wang S, Zhang X. 2020. Metabolic dysregulation contributes to the progression of Alzheimer's disease. Front. Neurosci. 14:530219.
72. Basun H, *et al.* 1990. Amino acid concentrations in cerebrospinal fluid and plasma in Alzheimer's disease and healthy control subjects. J Neural Transm Gen Sect 2:295–304.
73. Martinez M, Frank A, Diez-Tejedor E, Hernanz A. 1993. Amino acid concentrations in cerebrospinal fluid and serum in Alzheimer's disease and vascular dementia. J Neural Transm Gen Sect 6:1–9.
74. Hajjar I, Liu C, Jones DP, Uppal K. 2020. Untargeted metabolomics reveal dysregulations in sugar, methionine, and tyrosine pathways in the prodromal state of AD. Alzheimer's Dementia Diag Assess Dis Monitor 12:e12064.
75. Lodeiro M, Ibáñez C, Cifuentes A, Simó C, Cedazo-Mínguez Á. 2014. Decreased cerebrospinal fluid levels of L-carnitine in non-apolipoprotein E4 carriers at early stages of Alzheimer's disease. J Alzheimers Dis 41:223–232.
76. van der Velpen V *et al.* 2019. Systemic and central nervous system metabolic alterations in Alzheimer's disease. Alzheimer's Res Ther 11:93.
77. Czech C, *et al.* 2012. Metabolite profiling of Alzheimer's disease cerebrospinal fluid. PLoS ONE 7:e31501.
78. Mahajan UV, *et al.* 2020. Correction: dysregulation of multiple metabolic networks related to brain transmethylation and polyamine pathways in Alzheimer disease: a targeted metabolomic and transcriptomic study. PLoS Med 17:e1003439.
79. Trushina E, Dutta T, Persson X-MT, Mielke MM, Petersen RC. 2013. Identification of altered metabolic pathways in plasma and CSF in mild cognitive impairment and Alzheimer's disease using metabolomics. PLoS ONE 8:e63644.
80. Holmquist L, *et al.* 2007. Lipoic acid as a novel treatment for Alzheimer's disease and related dementias. Pharmacol Ther 113:154–164.
81. Haugaard N, Levin RM, Surname F. 2000. Regulation of the activity of choline acetyl transferase by lipoic acid. Mol Cell Biochem 213:61–63.
82. Bitar MS, Wahid S, Pilcher CW, Al-Saleh E, Al-Mulla F. 2004. Alpha-lipoic acid mitigates insulin resistance in Goto-Kakizaki rats. Horm Metab Res 36:542–549.
83. Lee WJ, *et al.* 2005. α-Lipoic acid increases insulin sensitivity by activating AMPK in skeletal muscle. Biochem Biophys Res Commun 332:885–891.
84. Thirunavukkarasu V, Nandhini AA, Anuradha CV. 2004. Lipoic acid attenuates hypertension and improves insulin sensitivity, kallikrein activity and nitrite levels in high fructose-fed rats. J Comp Physiol B 174:587–592.
85. Shrivastava SK, *et al.* 2019. Design and development of novel p-aminobenzoic acid derivatives as potential cholinesterase inhibitors for the treatment of Alzheimer's disease. Bioorg Chem 82:211–223.
86. Tajima Y, *et al.* 2013. Lipidomic analysis of brain tissues and plasma in a mouse model expressing mutated human amyloid precursor protein/tau for Alzheimer's disease. Lipids Health Dis 12:68.
87. Kumar D, Kumar P. 2019. An in-silico investigation of key lysine residues and their selection for clearing off Aβ and holo-AβPP through ubiquitination. Interdiscip Sci 11:584–596.
88. Kalia V, Jones DP, Miller GW. 2019. Networks at the nexus of systems biology and the exposome. Curr Opin Toxicol 6:25–31. DOI: 10.1016/j.cotox.2019.03.008. 2019 Apr 3.
89. Vermeulen R, Schymanski EL, Barabási A-L, Miller GW. 2020. The exposome and health: where chemistry meets biology. Science 367:392–396.
90. Rappaport SM, Barupal DK, Wishart D, Vineis P, Scalbert A. 2014. The blood exposome and its role in discovering causes of disease. Environ Health Perspect 122:769–774.
91. Mahmood SM. 2016. Toxicological and physiological effects of DDT on *Caenorhabditis elegans*. Ibn AL Haitham J Pure Appl Sci 24:89832025.
92. Muschiol D, Schroeder F, Traunspurger W. 2009. Life cycle and population growth rate of *Caenorhabditis elegans* studied by a new method. BMC Ecol 9:14.
93. Gibson GE, Sheu K-FR, Blass JP. 1998. Abnormalities of mitochondrial enzymes in Alzheimer disease. J Neural Transm 105:855–870.
94. Gibson GE, Park LCH, Zhang H, Sorbi S, Calingasan NY. 1999. Oxidative stress and a key metabolic enzyme in Alzheimer brains, cultured cells, and an animal model of chronic oxidative deficits. Ann NY Acad Sci 893:79–94.
95. Müller WE, Eckert A, Kurz C, Eckert GP, Leuner K. 2010. Mitochondrial dysfunction: common final pathway in brain aging and Alzheimer's disease—therapeutic aspects. Mol Neurobiol 41:159–171.
96. Yao J, *et al.* 2009. Mitochondrial bioenergetic deficit precedes Alzheimer's pathology in female mouse model of Alzheimer's disease. PNAS 106:14670–14675.
97. Ye X, Tai W, Zhang D. 2012. The early events of Alzheimer's disease pathology: from mitochondrial dysfunction to BDNF axonal transport deficits. Neurobiol Aging 33: 1122.e1–1122.e10.
98. Hauptmann S, *et al.* 2009. Mitochondrial dysfunction: an early event in Alzheimer pathology accumulates with age in AD transgenic mice. Neurobiol Aging 30:1574–1586.
99. Reddy PH, *et al.* 2004. Gene expression profiles of transcripts in amyloid precursor protein transgenic mice: up-regulation of mitochondrial metabolism and apoptotic genes is an early cellular change in Alzheimer's disease. Hum Mol Genet 13:1225–1240.
100. Croteau E, *et al.* 2018. A cross-sectional comparison of brain glucose and ketone metabolism in cognitively healthy older adults, mild cognitive impairment and early Alzheimer's disease. Exp Gerontol 107:18–26.
101. Butterfield DA, Boyd-Kimball D. 2018. Oxidative stress, amyloid-β peptide, and altered key molecular pathways in the pathogenesis and progression of Alzheimer's disease. J Alzheimers Dis 62:1345–1367.
102. Blass JP, Gibson GE. 1992. Nonneural markers in Alzheimer disease. Alzheimer Dis Assoc Disord 6:205–224.

103. Bosetti F, *et al.* 2002. Cytochrome c oxidase and mitochondrial F1F0-ATPase (ATP synthase) activities in platelets and brain from patients with Alzheimer's disease. Neurobiol Aging 23:371–376.
104. Curti D, *et al.* 1997. Oxidative metabolism in cultured fibroblasts derived from sporadic Alzheimer's disease (AD) patients. Neurosci Lett 236:13–16.
105. Swerdlow RH. 2011. Mitochondria and cell bioenergetics: increasingly recognized components and a possible etiologic cause of Alzheimer's disease. Antioxid Redox Signal 16:1434–1455.
106. Flannery PJ, Trushina E. 2019. Mitochondrial dynamics and transport in Alzheimer's disease. Mol Cell Neurosci 98: 109–120.
107. Sonntag K-C, *et al.* 2017. Late-onset Alzheimer's disease is associated with inherent changes in bioenergetics profiles. Sci Rep 7:14038.
108. Atlante A, de Bari L, Bobba A, Amadoro G. 2017. A disease with a sweet tooth: exploring the Warburg effect in Alzheimer's disease. Biogerontology 18:301–319.
109. Braungart E, Gerlach M, Riederer P, Baumeister R, Hoener MC. 2004. *Caenorhabditis elegans* MPP+ model of Parkinson's disease for high-throughput drug screenings. NDD 1:175–183.
110. Richardson JR, Quan Y, Sherer TB, Greenamyre JT, Miller GW. 2005. Paraquat neurotoxicity is distinct from that of MPTP and rotenone. Toxicol Sci 88:193–201.
111. David DC, *et al.* 2005. Proteomic and functional analyses reveal a mitochondrial dysfunction in P301L Tau transgenic mice. J Biol Chem 280:23802–23814.
112. Kim GW, Chan PH. 2001. Oxidative stress and neuronal DNA fragmentation mediate age-dependent vulnerability to the mitochondrial toxin, 3-nitropropionic acid, in the mouse striatum. Neurobiol Dis 8:114–126.
113. Lasagna-Reeves CA *et al.* 2011. Tau oligomers impair memory and induce synaptic and mitochondrial dysfunction in wild-type mice. Mol Neurodegen 6:39.
114. Shafiei SS, Guerrero-Muñoz MJ, Castillo-Carranza DL. 2017. Tau oligomers: cytotoxicity, propagation, and mitochondrial damage. Front Aging Neurosci 9:83.
115. Eckert A, Nisbet R, Grimm A, Götz J. 2014. March separate, strike together—role of phosphorylated TAU in mitochondrial dysfunction in Alzheimer's disease. Biochim Biophys Acta 1842:1258–1266.
116. Elmore SE, La Merrill MA. 2019. Oxidative phosphorylation impairment by DDT and DDE. Front Endocrinol 10:122.
117. Moreno AJ, Madeira VM. 1991. Mitochondrial bioenergetics as affected by DDT. Biochim Biophys Acta Bioenerget 1060:166–174.
118. Liu Q, *et al.* 2017. Organochloride pesticides impaired mitochondrial function in hepatocytes and aggravated disorders of fatty acid metabolism. Sci Rep 7:46339.
119. Eskenazi B, *et al.* 2006. In utero exposure to dichlorodiphenyltrichloroethane (DDT) and dichlorodiphenyldichloroethylene (DDE) and neurodevelopment among young Mexican American children. Pediatrics 118:233–241.
120. Du H, *et al.* 2015. Reproductive toxicity of endosulfan: implication from germ cell apoptosis modulated by mitochondrial dysfunction and genotoxic response genes in *Caenorhabditis elegans*. Toxicol Sci 145:118–127.
121. Bany IA, Dong M-Q, Koelle MR. 2003. Genetic and cellular basis for acetylcholine inhibition of *Caenorhabditis elegans* egg-laying behavior. J Neurosci 23:8060–8069.
122. Hooper DC, *et al.* 1998. Uric acid, a natural scavenger of peroxynitrite, in experimental allergic encephalomyelitis and multiple sclerosis. PNAS 95:675–680.
123. Wan Q-L, *et al.* 2020. Uric acid induces stress resistance and extends the life span through activating the stress response factor DAF-16/FOXO and SKN-1/NRF2. Aging 12: 2840–2856.
124. Rohn I, *et al.* 2018. Selenium species-dependent toxicity, bioavailability and metabolic transformations in *Caenorhabditis elegans*. Metallomics 10:818–827.
125. Hu X, *et al.* 2020. Metabolome wide association study of serum DDT and DDE in pregnancy and early postpartum. Reprod Toxicol 92:129–137.
126. Yan Q, *et al.* 2021. High-resolution metabolomic assessment of pesticide exposure in Central Valley, California. Chem Res Toxicol 34:1337–1347.
127. Wang C, Saar V, Leung KL, Chen L, Wong G. 2018. Human amyloid β peptide and tau co-expression impairs behavior and causes specific gene expression changes in *Caenorhabditis elegans*. Neurobiol Dis 109:88–101.
128. Zarse K, Schulz TJ, Birringer M, Ristow M. 2007. Impaired respiration is positively correlated with decreased life span in *Caenorhabditis elegans* models of Friedreich Ataxia. FASEB J 21:1271–1275.
129. Maglioni S, Mello DF, Schiavi A, Meyer JN, Ventura N. 2019. Mitochondrial bioenergetic changes during development as an indicator of *C. elegans* health-span. Aging 11: 6535–6554.
130. Wytock TP, *et al.* 2020. Extreme antagonism arising from gene-environment interactions. Biophys J 119:2074–2086.
131. Bloomquist JR. 1996. Ion channels as targets for insecticides. Annu Rev Entomol 41:163–190.
132. Narahashi T. 2000. Neuroreceptors and ion channels as the basis for drug action: past, present, and future. J Pharmacol Exp Ther 294:1–26.
133. Hobert O. 2018. The neuronal genome of *Caenorhabditis elegans*. The C. elegans Research Community, WormBook. http://www.wormbook.org.
134. Frigo DE, Burow ME, Mitchell KA, Chiang T-C, McLachlan JA. 2002. DDT and its metabolites alter gene expression in human uterine cell lines through estrogen receptor-independent mechanisms. Environ Health Perspect 110 :1239–1245.
135. Lühmann K, *et al.* 2020. Environmental pollutants modulate transcriptional activity of nuclear receptors of whales in vitro. Environ Sci Technol 54:5629–5639.
136. Hall JM, Greco CW. 2020. Perturbation of nuclear hormone receptors by endocrine disrupting chemicals: mechanisms and pathological consequences of exposure. Cells 9:13.
137. Gissendanner CR, Crossgrove K, Kraus KA, Maina CV, Sluder AE. 2004. Expression and function of conserved nuclear receptor genes in *Caenorhabditis elegans*. Dev Biol 266:399–416.